Ultrasound Localization Microscopy and Super-Resolution: A State of the Art

Olivier Couture, Vincent Hingot, Baptiste Heiles, Pauline Muleki-Seya, and Mickael Tanter

***Abstract*— Because it drives the compromise between resolution and penetration, the diffraction limit has long represented an unreachable summit to conquer in ultrasound imaging. Within a few years after the introduction of optical localization microscopy, we proposed its acoustic alter ego that exploits the micrometric localization of microbubble contrast agents to reconstruct the finest vessels in the body in-depth. Various groups now working on the subject are optimizing the localization precision, microbubble separation, acquisition time, tracking, and velocimetry to improve the capacity of ultrasound localization microscopy (ULM) to detect and distinguish vessels much smaller than the wavelength. It has since been used *in vivo* in the brain, the kidney, and tumors. In the clinic, ULM is bound to improve drastically our vision of the microvasculature, which could revolutionize the diagnosis of cancer, arteriosclerosis, stroke, and diabetes.**

***Index Terms*— Angiography, microbubbles, super-resolution, ultrasound localization microscopy (ULM).**

I. Ultrasound Imaging: Lower Frequency Means More Penetration

SCIENCE is guided by our quest for studying and understanding the invisible. Through history, the invention of instruments to distinguish objects that are too small or hidden to the naked eye has led to new understanding of matter and life. Optical microscopy, for instance, was invented four centuries ago and has been essential to the discovery of cellular processes and pathogens, thus indirectly saving hundreds of millions of lives. It benefits from a spatial resolution, the capacity to distinguish close objects, in hundreds of nanometers. It is only limited by its wavelength by diffraction. However, optical microscopy is generally bound to shallow specimen due to its lack of penetration. When applied to human health, these microscopes remain the gold standard for the diagnosis of many diseases, such as cancer, through histopathology.

The opacity of the human body to light, nonetheless, has justified the invention of imaging modalities that can observe the organs of interest through several centimeters of tissue. X-ray, ultrasound, magnetic resonance imaging (MRI), positron emission tomography, and computed tomography are now common household names, each applied differently due to their respective tradeoffs between resolution, contrast source, penetration, sensitivity, frame rate, full-body nature, cost, and availability. Nevertheless, none of these medical imaging techniques has approached the resolution of optical microscopy in depth, either because of a fundamental compromise due to diffraction, as in ultrasound imaging, or through a more complex consideration such as radiation dose, acquisition time, or mean-free particle path.

More than 70 years after its birth [2]–[4], ultrasound imaging remains a key modality for observing the heart, liver, kidneys, breast, testis, prostate, thyroid, muscles, vascular structures, and the human fetus. Helped with its excellent spatial resolution (few hundred micrometer) and time resolution (tens of frames per second), conventional ultrasound provides a window in soft tissue that guides diagnosis, prognosis, and interventions in hospitals throughout the world [5]. For physiological imaging, standard B-mode images can be overlaid with pulsed-Doppler which provides maps of blood vessels with flows beyond a few centimeter per second. Doppler is a key component of most ultrasound exams today, as it yields information on the organs function, and not just their anatomy.

As conventional Doppler ultrasound relies on the rapid displacement of red blood cells to detect them with respect to tissue, slow flow remained difficult to observe. The discovery of ultrasound contrast agents by Gramiak *et al.* [6] allowed the indirect observation of the smallest vessels through the detection of intravascular microbubbles. Even in relatively small concentrations (in the order of 1 per 10^5 red blood cells), injected bubbles of air, or perfluorocarbon, a few micrometers in size increase the intensity of blood vessels by more than a factor of a hundred. This is due to impedance mismatch between blood and gas, but also by the resonance of these natural oscillators [7]. Moreover, microbubble oscillation can become nonlinear at clinically relevant acoustic pressure range, helping their detection with respect to mostly linear tissue [8]. When a certain threshold is attained, these contrast agents can also be disrupted by ultrasound, enabling differential imaging. In fact, ultrasound is so sensitive to pockets of gas that single microbubbles can be detected [9]. Microbubbles greatly enhance the perfusion of liver tumor [10], prostate tumor [11], or myocardium [12] in clinical settings.

Beyond microbubbles, research in ultrasound imaging is undergoing a paradigm shift with the availability of the ultrafast programmable ultrasound scanner. By using plane-wave emissions rather than line-by-line pulse echo, frame

Manuscript received April 12, 2018; accepted June 21, 2018. Date of publication June 26, 2018; date of current version July 30, 2018. This work was supported by the Agence Nationale de la Recherche through the Project ANR Tremplin, and by LABEX WIFI (Laboratory of Excellence) through the French Program "Investments for the Future" under Reference ANR-10-LABX-24 and Reference ANR-10-IDEX-0001-02 PSL*. *(Corresponding author: Olivier Couture.)*

The authors are with ESPCI Paris, Paris Sciences et Lettres Research University, CNRS, INSERM, Institut Langevin, 75012 Paris, France (e-mail: olivier.couture@espci.fr).

Digital Object Identifier 10.1109/TUFFC.2018.2850811

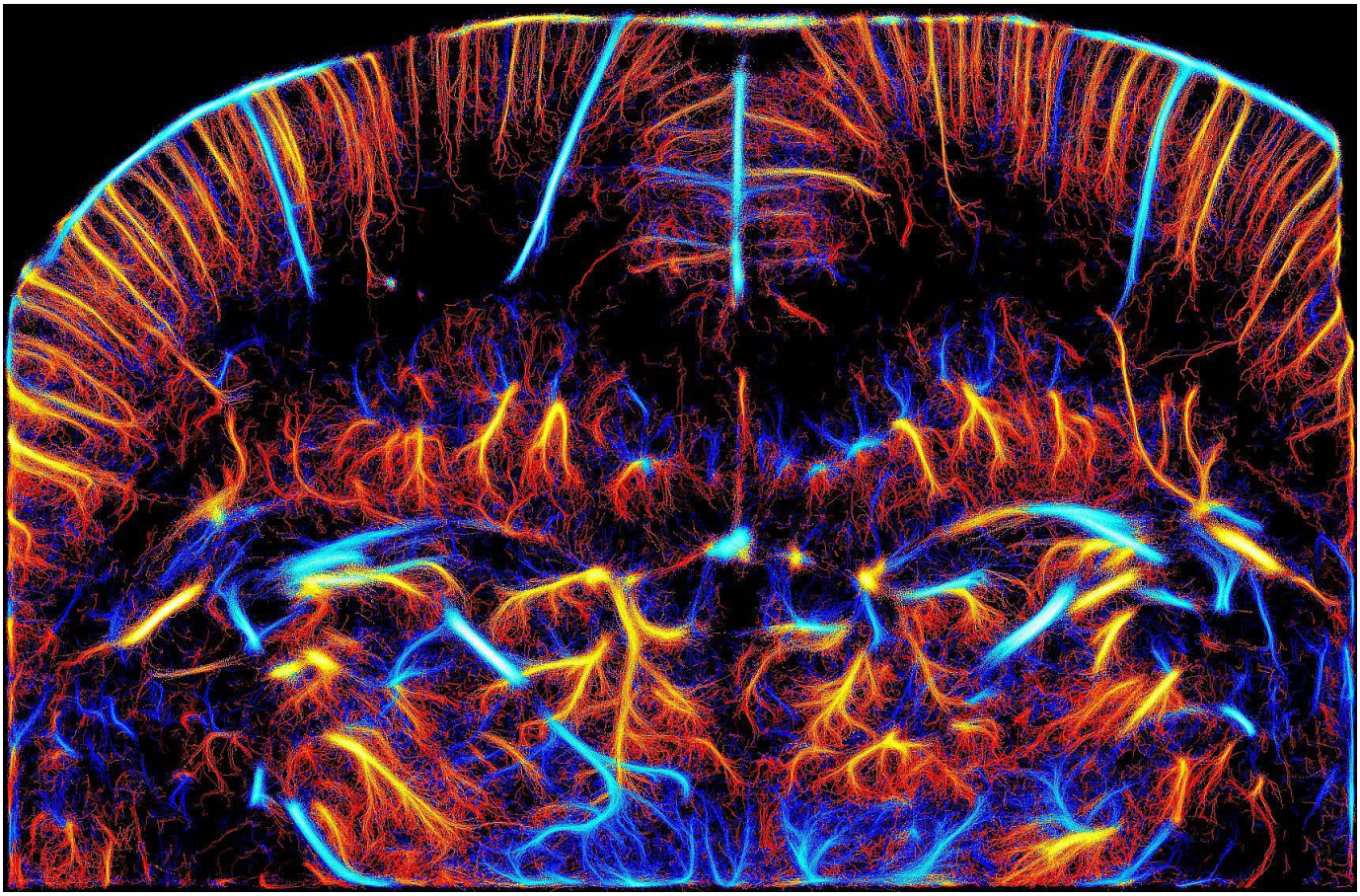

Fig. 1. ULM of the living rat brain (reconstructed from data in [1]).

rates were increased from 50 to 20 000 Hz giving access to rapid phenomena [13]. The concept of ultrafast ultrasound, denominated and initiated in the 1970s [14], [15], has found its first clinical application with transient elastography [16] and shear wave elastography [17], which demonstrated that the elasticity of tissue can be mapped and quantified in-depth to help the diagnosis of breast cancer [18] and liver fibrosis [19], for example. The accumulation of thousands of ultrasound images at ultrafast frame rates also allows the observation of slow processes, such as blood flow in the millimeter per second range [20]. This is due to the increased amount of data and to the possibility to use more efficient filters on long ensembles of images such as singular value decomposition (SVD) [21] in order to unambiguously discriminate tissue motion and very slow blood flows. This increase of sensitivity by more than an order of magnitude gives new information on blood flow in various organs, including newborn brains [22]. It opened an entirely new field with functional ultrasound [23], [24], which can map the neuronal brain activation of free-moving animals [25], [26], human newborns [27], and during brain surgery in adults [28]. The combination of ultrafast imaging and microbubbles was also shown to be fruitful since it reduces microbubble disruption for an enhanced contrast [29], [30]. Moreover, Doppler sequences can be easily interleaved with ultrafast nonlinear pulses [31]. It also permitted transcranial ultrasound functional imaging [32]. Moreover, it can provide higher contrast-to-tissue ratio (CTR) than nonlinear methods even in a clinical setting for microbubbles moving faster than a few millimeters per second [33]. We shall see below that it can do much more (Fig. 1).

Beyond frame rates, the introduction of software-based ultrasound scanners has opened new possibilities in ultrasound research laboratories, allowing the rapid introduction and *in vivo* testing of new sequences. Rather than modifying the electronic hardware, we can now rapidly modify parameters of emission, reception, and beamforming to yield new types of contrast, a freedom that MRI-scientists have enjoyed for many years now. With the help of the ultrafast programmable ultrasound scanner, we expect the blossoming of many ultrasound-based techniques in the near future [34]–[36].

However, even at 20 000 frames/s, ultrasound imaging remains bound to diffraction due to its undulatory nature and is confined by the compromise between penetration and resolution. For instance, cardiac imaging performed at 3 MHz to achieve a penetration of 15 cm will be limited to a 1-mm resolution in practical conditions (Fig. 2). It can be improved through harmonic imaging [37], but resolution remains bound to the submillimetric regime. Indeed, the resolution of ultrasound is defined by diffraction, which eliminates, in the far-field, aspects that are smaller than approximately a half-wavelength. For instance, the lateral resolution is linked to

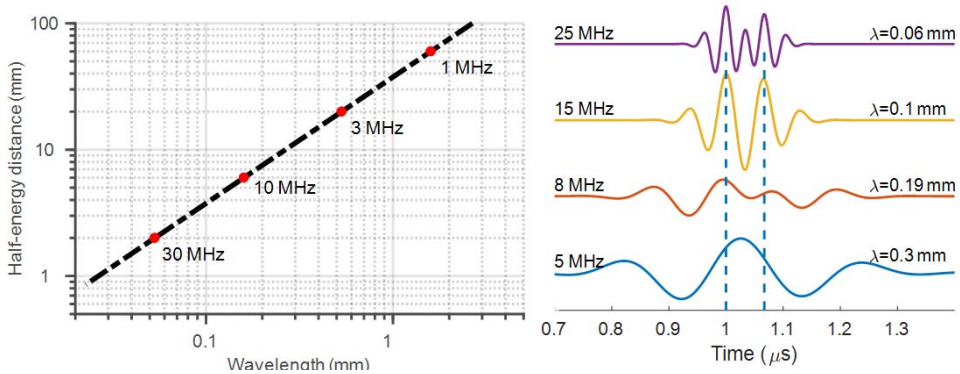

Fig. 2. Compromise between resolution, defined by the wavelength and ultrasound penetration (left). The half-energy distance corresponds to a loss of 3 dB in liver tissue (attenuation $\approx$ 0.5 dB/cm/MHz, extrapolated linearly from [38]). Separability of two sources (dotted lines), 0.1 mm apart, using acoustic pulses emitted at various wavelengths (60% bandwidth) (right). The sources are indistinguishable when they are closer than a half-wavelength.

the full-width at half-maximum (FWHM) of the point-spread function [5]: FWHM $= 1.4\,\lambda F/D$, where λ is the wavelength, F is the focal length, and D is the aperture. Knowing that the attenuation of ultrasound in tissue also depends on frequency, with a relationship of $f^{1\,\text{to}\,2}$ (where $\lambda = c/f$, where c is the speed of sound and f is the frequency), it is clear that a better resolved image will be generally achievable at a shallower depth. Therefore, the resonant frequency of the piezoelectric crystal, the choice of the probe and, sometimes, the electronics, is bound by this compromise between resolution and penetration, restricting the options for radiologists and researchers alike.

II. Better Resolved Ultrasound

Several approaches have been proposed to improve the resolution of ultrasound imaging. Increasing the frequency is the most direct possibility [39]. Exploiting scanners using pulses beyond 15 MHz for high-frequency ultrasound gives access to resolution below 100 μm. But for a 100-dB dynamic range, the maximum imaging depth is about 300 wavelengths, which limits penetration to 30 mm at 15 MHz and 10 mm at 35 MHz [40]. High-frequency ultrasound is now widespread in animal models and can be used to observe implanted tumors [41], cardiac imaging [42], fetal development [43], and many other applications. In human applications, it can be used for intravascular ultrasound with the exploitation of a catheter-based ultrasonic probe [44].

An important step toward higher resolutions was achieved with the development of ultrasound angiography [45], [46]. This technique uses the very high ultraharmonics (10th harmonic or higher) emitted by microbubbles after insonification at relatively low frequencies (2.25 MHz, for example) to reconstruct images of vessels. This means that the propagation length at the highest frequency is halved, improving the compromise between resolution and penetration. This technique, which required dual-transducer technology, was applied to the imaging of subcutaneous tumor models.

Nevertheless, ultrasound angiography and high-frequency ultrasound remain limited to the diffraction limit as they simply exploit shorter wavelengths to create images. In this review, we shall define super-resolution ultrasound as a technique that surpasses the classical limit of diffraction for imaging and allows the detection and separation of subwavelength features. In general, the separability of two objects or structures distant by less than half of the minimum wavelength is considered appropriate criteria for super-resolution.

The diffraction limit is applicable in the far-field, and an elegant way to bypass this compromise is to perform imaging in the near field. Less than a few wavelengths away from a probe, evanescent waves allow the observation of structures that are in the order of the distance between the instrument and the object [47]. This subtends ultrasound microscopy, where the acoustical waves is generated and detected within a micrometer or less from the sample. It can map acoustical contrast, linked to the density, and compressibility of objects at a nanometric scale. However, in medical imaging, organs are often at hundreds of wavelengths from the probe and near-field super-resolution techniques are difficult to apply.

Another way to achieve super-resolution for other contrasts such as optical absorption, shear modulus, or dielectric permittivity is to exploit the interactions between ultrasound and other waves of different nature. In this approach, called multiwave imaging [48], ultrasound is often used to improve the conventional resolution provided by other types of waves; optical waves in photo-acoustics, shear waves in elastography, or electromagnetic waves in acoustoelectric imaging. For practical reasons, we will restrict this review to the single use of ultrasonic waves for far-field imaging.

The development of metamaterials has also introduced new ideas around super-resolution by allowing super-focusing in the near field of resonant heterogeneities with electromagnetic waves [49]. The idea is inspired by Pendry's "perfect lens" with doubly negative material [50]. In ultrasound, such materials known as phononic crystals were shown to achieve resolutions close to $\lambda/3$, which is better than the diffraction limit [51], [52].

Closer to the concept of localization, super-resolution ultrasound was also shown to be achievable when a limited number of scatterers are present in the observed medium [53], [54]. Through a combination of maximum-likelihood and multiple signal characterization (MUSIC) and decomposition of the time-reversal operator (DORT), Prada and Thomas [55] were able to demonstrate experimentally subwavelength localization of scatterers when the number of these scatterers was smaller

than the number of array elements. In particular, they were able to separate two point-like scatterers $\lambda/3$ apart in the far-field. It required several realizations, beyond the number of scatterers to be separated. Unfortunately, from an acoustic point of view, the nature of biological tissues inherently corresponds to a random distribution of millions of spatially unresolved Rayleigh scatterers (the so-called "speckle noise") whose number is orders of magnitude larger than the limited number of independent ultrasonic transmitters composing an ultrasonic imaging scanner. Thus, all these methods were unlikely to be achievable in a fully developed speckle in ultrasound imaging as the scatterers are considered innumerable. However, a very interesting insight from these researchers was that super-resolution is possible in ultrasound imaging if a restricted number of scatterers is detectable.

Other approaches to achieve a form of super-resolution exploit strongly conditioned *a priori* information on the object or the insonification pattern. For instance, Clement *et al.* [56] described an experiment where known single wires could be measured with a thickness much smaller than the wavelength. An approach exploiting the Moiré effect from multiple ultrasonic beams was also introduced as acoustical structured illumination by Ilovitsch *et al.* [57]. With multiple emissions of shifted patterns, they were able to improve the resolution of the image by a factor of 2. However, it requires a precise *a priori* calculation of the phase of the propagating field.

Hence, the field of super-resolution ultrasound is several decades old [58], [59] and its development remained sparse until recently due to the incapacity of ultrasonic waves to separate the signature of millions of randomly distributed scatterers and without a strong *a priori* information. It took a revolutionary development in the field of optics, an undulatory close-kin to ultrasound, to create a new excitement for super-resolution ultrasound, namely, localization microscopy.

III. Optical Res/Volution

Even with the introduction of these various approaches to breach the diffraction limit, the applicable resolution of ultrasound imaging remained, until recently, desperately wavelength-like. This situation has also plagued optical microscopy in the past, which has also seen numerous examples of near-field approaches [60], metamaterials concept [61], structured illumination [60], [62], and other processes to defeat their diffraction limit of a few hundred nanometers. This state of affair was revolutionized by optical localization microscopy [63] whose implications and applications created sufficient ripple for the 2014 Chemistry Nobel Prize to be awarded to Eric Betzig, Stefan Hell, and William E. Moerner [64].

Biological applications of optical microscopy rely heavily on fluorescent tiny beacons within the observed object [65], which are used to label every aspect of molecular pathways, antibodies, and genetic materials. Reporter genes inducing the production of fluorescent proteins have revolutionized genetics, also yielding a Nobel Prize in 2008 [66]. As demonstrated by Moerner and Kador [67] and Betzig and Chichester [68], optical microscopes are sufficiently sensitive to detect single fluorescent labels.

The nonlinear response of certain fluorescent labels can allow the restriction of the focal spot within a fraction of the wavelength, such as in the stimulated emission depletion (STED) technique [69]. This technique which exploits the selective deactivation of fluorophores within a doughnut-shape surrounding the observation spot can achieve resolutions in the order of tens of nanometer [70]. Even with the necessary beam scanning, it can achieve up to 200 frames/s in optimal conditions [71].

The stochastic blinking of fluorescent labels observed over large numbers of frames can also be used to increase resolution. In photoactivated localization microscopy (PALM) [63], fluorescence PALM (FPALM) [72], or stochastic optical reconstruction microscopy (STORM) [73], fluorescent labels switch between bright and dark states, making it such that only a subset of them are observable in each image [74]. Due to the limited number of sources in each image, the responses of the fluorescent labels do not interfere with each other. Consequently, it is possible to deconvolve the point spread function of the system from the image and determine the centroid of the sources with a localization precision much higher than the wavelength [75]. FPALM, PALM, and STORM exploit this blinking to accumulate the localization of point sources over thousands of images to recreate a super-resolved image. Betzig *et al.* [63] demonstrated that the error on the fitted position is dependent on "the standard deviation of a Gaussian approximating the true PSF" and inversely correlated with the square root of the number of detected photons from the source. More than 10 000 photons can be collected from single sources, yielding a potential resolution of 1 nm for a wavelength of a few hundred nanometers. In practical situations, the resolution is within tens of nanometers, which is already an order of magnitude better than the wavelength. However, accumulation time and damaging fluence can be detrimental.

In general, PALM requires several conditions [76].

1) *Sensitivity:* A sensitivity allowing the detection of labels that are much smaller than the wavelength (1/1000).
2) *Localization:* The positioning of these labels with a precision better than the diffraction limit.
3) *Video Recording:* Multiframe acquisition at a relatively high frame rate.
4) *Isolated Sources in a Spatiotemporal Referential:* A switchable label to restrict their local concentration at a specific time point in order to ensure the possibility of localizing them.

For FPALM, these conditions were achieved with switchable fluorescent labels and video cameras connected to the optical microscope.

Super-resolution optical fluctuation imaging (SOFI) also exploits the blinking of fluorescent sources and a video recording to increase the resolution of optical microscopy [77]. However, it relies on the higher order statistics of temporal fluctuations rather than localizing individual sources. Because the spatial distribution of cumulants from the image series narrows as the order of cumulants increases, a superior resolution

can be attained. This technique is significantly more rapid than PALM and it requires less fluence. However, it yields a limited improvement of the resolution dependent on the square root of the cumulant order and noise can become detrimental in imaging applications beyond the second order [78].

As demonstrated by the attribution of the Nobel Prize, the field of optics and its biological applications benefited enormously from the development of super-resolution microscopy [79]. Biological processes at the scale of the nanometers, such as adhesion dynamics [80], single-molecule trajectories [81], or microtubules organization [82], are now accessible.

IV. Ultrasonic Replication

Within five years after Betzig *et al.*'s [63] paper, our team proposed to apply equivalent approaches to exploit localization microscopy in ultrasound [83], [84]. The suggested idea was to use ultrasound contrast agents as the punctual sources and ultrafast imaging of their disruption or movement as the necessary state fluctuation in the backscattered signals. Indeed, the important idea that ultrafast differential imaging was able to catch very transient fluctuations had recently been demonstrated for the estimation of the fast dissolution dynamics of microbubbles after disruption in [29] and for the estimation of the *in vivo* cavitation threshold by tracking the appearance of a single cavitation bubble in the brain [85]. For ULM, the general principle is to emit an ultrasonic pulse in a medium that contains microbubbles and collect the received echo. In the matrix of radio frequency (RF) data acquired by each channel (number of samples x number of elements), single echoes of microbubbles propagating at a constant speed of sound (c) are represented by hyperbolas described by the time of flight to arrive at each transducer element. If this echo is unique, a simple fit can provide the position of the microbubbles with a much higher resolution than the wavelength. Even if the echo is beamformed by a clinical scanner, a process that converts the hyperbola on RF channel data into a point in an image, the centroid of the microbubble can be defined very precisely for stand-alone sources. As in optics, the question is never if wave-based imaging methods can precisely localize individual sources, but rather how to obtain these punctual sources in the first place!

As we have seen, methods initiated decades before, such as MUSIC, could already claim the name of super-resolution ultrasound but for a very limited number of scatterers which does not correspond to the configuration of biomedical ultrasound. The innovation can be rather seen as the introduction of ultrasound localization microscopy (ULM), a direct pendant to PALM, leading to super-resolution in configurations where millions of scatterers are present. ULM can mirror the conditions for PALM adapted from von Diezmann *et al.* [76] and some are even more favorable in acoustics than in optics.

1) *Sensitivity:* The sensitivity of ultrasound to its contrast agents, microbubbles, is extremely high as it was already described that single microbubbles a few micrometers in diameter (λ/100) can be imaged with a clinical scanner [9]. This is due to their impedance mismatch, resonance in the megahertz range and nonlinearities. Contrary to optical agents, they can be detected at several centimeter depths in tissue, making them a clinically relevant contrast modality. These isolated microbubbles are often seen at the beginning and end of the injected boluses in the clinic. The tracks of individual bubbles could even be superposed to create maximum intensity projection images, which remained, however, diffraction limited [86]. Initially, it may appear restricting to use blood-pool microbubbles as the labels for ultrasound super-resolution. However, a vast number of diseases involve the microvasculature, such as cardio- and cerebrovascular diseases, cancer, and diabetes. Currently, hundreds of thousands of contrast-enhanced ultrasound scans are performed every year, in addition to the millions of Doppler exams.
2) *Localization:* Because ultrasonic waves remain coherent when propagating into tissue and that our acquisition systems are sensitive to phase, minute decorrelations much smaller than the wavelength (λ/100 or less) can be observed with an ultrasound scanner. This sensitivity to small changes is exploited in Doppler imaging [87], but also by displacement measurements [88] and transient elastography which can detect vectorial displacements in the range of micrometers at kilohertz frame rates [17]. Moreover, the response of ultrasound images to a single isolated point is well behaved and well known (point-spread function [5]). Ultrasound can be refocused even through highly aberrating [36], [89], multiply scattering [90], and even nonlinear media [91]. From the response of a single isolated microbubble, we can thus pinpoint its centroid with a resolution much greater than the wavelength, as it was demonstrated for other strong scatterers with DORT and MUSIC [55].
3) *Video Recording:* Conventional ultrasound is already the fastest clinical imaging modality with frame rates around 50 frames/s. In the "M-mode" (single line imaging), phenomena in the timescale of the pulse echo (less than 100 μs) can also be detected over a single line. Ultrafast imaging pushed these frame rates by a few order of magnitude by producing entire frames within one pulse echo (up to 20 000 frames/s for shallow tissue). Planar [92] or volumetric [93] compounding has allowed a direct tradeoff between image quality and frame rates. The exponential development of RAM and graphical processing units also permits the accumulation and beamforming of millions of images within one acquisition. Far beyond just a technological leap, such ultrafast frame rates are a key for ULM as tiny *in vivo* tissue motion or even physiological tissue pulsatility occurring at tens of micrometers and millisecond ranges can destroy our ability to produce microscopic images if uncorrected.
4) *Isolated Sources in a Spatiotemporal Referential:* The principle of localization microscopy is that sources are isolated in each individual image. For localization to work precisely, isolated sources such as microbubbles need to be separated by a wavelength or more. Indeed,

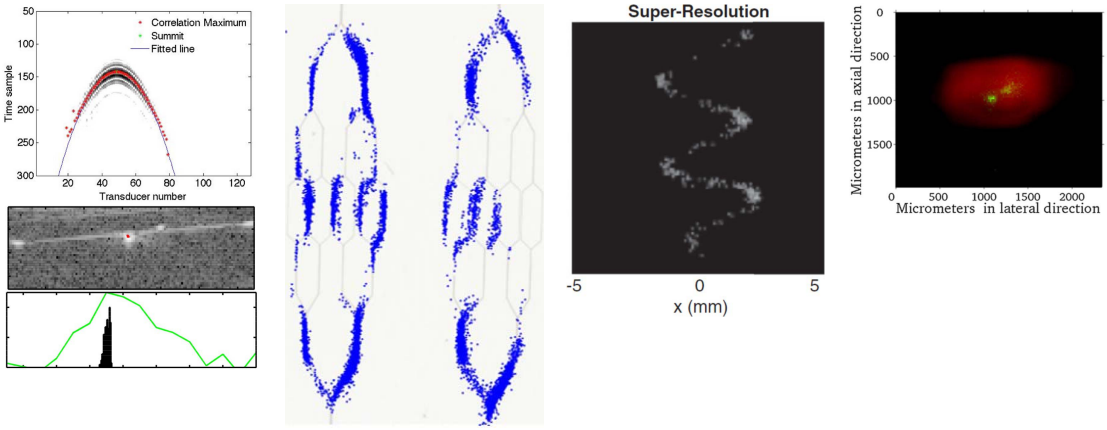

Fig. 3. First examples of *in vitro* ULM. (a) Ultrafast localization of microbubbles in a liquid and in a tube (© 2011 IEEE. Reprinted, with permission, from [83]). (b) 3-D ULM in microfluidics channels (reproduced from [97] with the permission of AIP publishing). (c) 3-D low-concentration microbubble localization in a tube (reproduced from [96] by permissions of Wiley company, all rights reserved). (d) Planar low-concentration nonlinear localization of microbubbles in two tubes (reproduced from [95], © Institute of Physics and Engineering in Medicine. Reproduced by permission of IOP Publishing. All rights reserved).

in a single image, the PSF of two microbubbles should not be superposed by more than 50% in order to fulfill the Rayleigh criteria and avoid the bias in the localization of their respective centroid (Fig. 2). One of the main questions of the current developments in super-resolution ultrasound is the method by which microbubbles are separated. The most straightforward answer consists of using a very limited concentration of microbubbles. Indeed, when injected at standard concentration (a few hundred million bubbles in a human) at the peak of the bolus, several microbubbles are present in each pixel at clinical frequencies making them impossible to distinguish. Drastically reducing the concentrations leads to a separability between individual microbubbles which can then be individually localized. In the case of large microbubble clouds (high concentration), ultrafast imaging solves the problem of individual bubble separation by detecting their transient individual signatures from the decorrelation of successive ultrasonic backscattered signals. This decorrelation can be due to movement or disruption. However, with the advent of tracking methods, the disruption of microbubbles is detrimental and low mechanical index pulses should rather be used to observe microbubbles as they individually flow through microvessels.

With the exception of ultrasonic transposition of SOFI [94], which will be discussed below, ultrasonic super-resolution techniques introduced recently for *in vivo* imaging are ULM methods. In our view, to prevent confusion with MUSIC, near-field methods, structured illumination, or higher order statistics fluctuation-based methods, the technique should be described generally as ULM rather than super-resolution ultrasound. Indeed, localization is the key concept required to reach at least one or two orders of magnitude improvement of the ultrasonic resolution compared to the wavelength and leading to microscopic resolution. Resulting images can be referred as super-resolved, but the method is based on localization.

V. Technical Developments in Ultrasound Localization Microscopy

Initially, ULM has been described *in vitro* in microvessel phantoms [83], [95]–[97]. In the initial demonstration of ultrafast ULM, Couture *et al.* [83] described the error in the localization of large floating isolated microbubbles with ultrafast imaging, and showed a $\lambda/250$ resolution in the axial direction. Second, it showed the precise localization of microbubbles contrast agents in polydimethylsiloxane microchannels, which demonstrated a clear reduction in the apparent size of tube [Fig. 3(a)]. Finally, Couture *et al.* [83] observed individual microbubble events linked to the decorrelation of contrast agents during contrast imaging of implanted tumors with an ultrafast scanner. This study used the fitting of the individual microbubble echo on channel RF data to localize the microbubbles. Fitting of hyperboloid echoes on the RF data allows the exclusion of outliers and phase jump which cannot be retrieved from beamformed images.

In parallel to this first demonstration of ULM, Siepmann *et al.* [98] described a centroid detection of dilute microbubbles for the improvement of maximum intensity projection images. They demonstrated this strategy in tumor mouse models mapped with a high-frequency ultrasonic scanner. More than a super-resolution technique, they describe their strategy to determine precisely the local microbubble density, which could give additional information on tumor perfusion. They exploited motion correction and foresaw improvement through tracking in their discussion.

Following these initial studies, the year 2013 saw the publication of three founding articles on ULM by independent groups. Viessman *et al.* [95] performed localization microscopy of microtubes in 2-D using a conventional scanner showing that two touching 200-μm vessels could be distinguished with the method [Fig. 3(d)]. They discriminated microbubbles from each other through the dilution of the microbubbles. The authors exploited nonlinear imaging to extract microbubbles from tissue, using a clinically applied

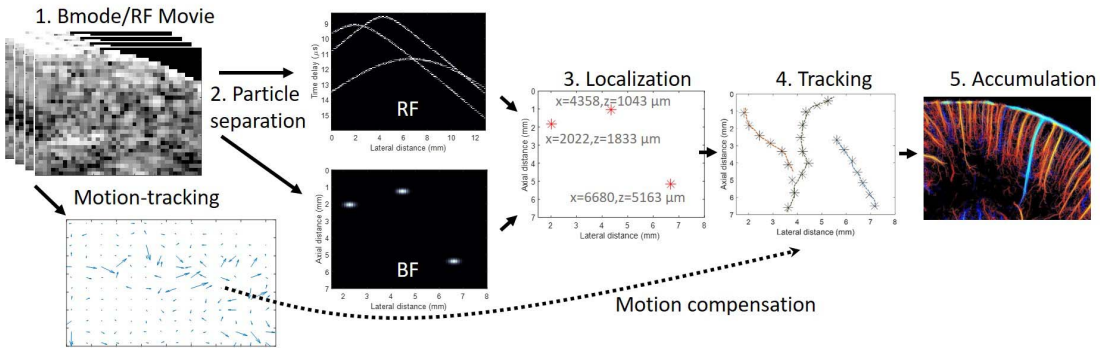

Fig. 4. General steps for ULM. 1) 100s to 100 000s of images or RF channel matrices are acquired and stacked. 2) Slow-time filtering or low concentration allows the separation of particles/microbubbles. 3) Centroids of the hyperbolas or the focal spots created by the microbubble are localized. 4) Localization of microbubbles is assigned to tracks to determine the velocity vector. 5) Resulting tracks through the movie are accumulated in one image. In parallel, motion is tracked in the cineloop and used to correct microbubble localization.

mode [contrast harmonic imaging (CHI)]. The wavelength of the received echo was approximately 300 μm, but the authors obtained a localization precision down to 2 μm using a brass wire.

A 3-D super-resolution approach was presented by O'Reilly and Hynynen [96] using a hemispherical array used in therapeutic ultrasound [Fig. 3(c)]. This application appears particularly promising in the context of the development of blood-brain barrier opening techniques exploiting microbubbles. They also showed that the localization of individual microbubbles can map microtubes behind the skull. The separation of microbubbles was also performed through the dilution of the contrast agent.

Finally, our group generalized the initial work on ultrafast ULM in 3-D by using a 1.5-D array to reconstruct the super-resolved position of microbubbles in the axial, lateral but also elevation directions [Fig. 3(b)] [97]. Ultrafast imaging was still implemented and decorrelation through differential filters was exploited to separate microbubbles present in high concentrations. The technique allowed, at a frequency of 1.75 MHz ($\lambda = 850$ microns), the reconstruction of a branching vascular network in a microfuidics phantom with channels as small as 40 μm ($\lambda/20$).

Within these five initial studies, most of the elements of ULM were already in place. In general, such acquisitions follow these steps (Fig. 4).

1) An injection of a contrast agent at a low ($\sim 10^6$ microbubbles injected) or a high concentration ($\sim 10^8$ microbubbles).
2) A video acquisition of a 100 to a 100 000 B-mode with or without contrast-specific pulse sequences, at conventional or ultrafast frame rate.
3) A motion correction algorithm.
4) A filtering step highlighting distinct individual microbubbles on each.
5) The localization of the centroid of each of the microbubble echo in the RF field or on beamformed images. Thousands to tens of millions of microbubbles can be localized over a cineloop.
6) The tracking of the localized points to define the paths of microbubbles in microvessels.
7) The visualization of the accumulation of individually localized microbubbles, their density, or their calculated velocities.

Each of these steps was optimized by various groups, several tradeoffs were discovered, and numerous strategies were introduced to circumvent them. However, it is important to note that the resulting resolutions have varied drastically between groups, even if they all claimed to defeat the diffraction limit. In some cases, authors have shown an improvement by more than one order of magnitude, others have achieved a small gain with respect to the half-wavelength limits, and for others, it suffices to supplant the FWHM $= 1.4\ \lambda F/D$. In the end, resulting images can only be compared on the basis of the subwavelength structures that can be detected and separated. For instance, channels much closer than the wavelength can be shown to be separated with ULM [95]–[97]. Further down the tracking process, the vectorial information obtained from ULM can be used to determine the statistical significance of the difference between the velocities in two subpixels in order to determine the ultimate resolution [99].

The following developments in 2015 involved the technology transfer to the *in vivo* setting (more in the dedicated section below), but continuing work on the optimization of ULM remained important. It was essential, for instance, to theoretically predict the maximum resolution achievable by this technique and under what conditions. This lower bound is defined by the localization precision of each microbubble, and it is linked to the minimal temporal delay which can be estimated between similar echoes, the so-called Cramer-Rao lower bound [88]. The theoretical resolution limit achievable in ULM was given in [99] and shown to present nice analogies with the resolution limit in optical localization microscopy. This theoretical resolution limit was demonstrated and validated experimentally by Desailly *et al.* [100]. The process of localization on the hyperboloid echoes in the RF channel data or determining the centroid on beamformed data are similar as they relate to the fitting of the time-of-flight equation with respect to the localization of the source and of the transducers. However, the equivalency between the localization in the RF space and the beamformed space might be affected by nonlinear processing such as the correction of outliers and

phase jumps in the fitting of the microbubble echo. A recent article by Song *et al.* [101] has described the influence of the spatial sampling of the beamforming on the localization error.

In the far-field, Desailly *et al.* [100] showed that the achievable resolution was (1) in the lateral and (2) in the axial resolution, where σ_τ is the standard deviation of the position of the echo time on each channel RF line, n is the number of transducer elements, c is the speed of sound z_0 the depth, and L is the size of the array. This shift depends on the pulse bandwidth, the pulse center frequency, the SNR, and finally the temporal jitter between electronic channels of the scanner whose classical values (2–6 ns) sets an intrinsic limit to some micrometer resolution. Interestingly, these equations relate very well to the maximum resolution in FPALM which is highly dependent on s, the standard deviation of a Gaussian approximating the true Paris Sciences et Lettres and N, the total number of detected photons (3). In practice, the model predicted an axial resolution of approximately 2 μm at 7 MHz. An interesting coincidence is that this limitation correspond approximatively to the size of the microbubble, linking the geometric confinement of the microbubble to the ultrasound capacity at localizing them

$$\sigma_{\hat{z}_0} \approx \frac{c.\sigma_\tau}{2.\sqrt{n}} \tag{1}$$

$$\sigma_{\hat{x}0} \approx 2\sqrt{3}.\frac{c.\sigma_\tau.z_0}{\sqrt{n}.L_x} \tag{2}$$

$$\sigma_{x,y} \approx \frac{s}{\sqrt{n}}. \tag{3}$$

Apart from the precision of localization, the first question in ULM is often how to distinguish the microbubbles from surrounding tissue, which was thoroughly studied in the field of contrast-enhanced ultrasound [102]. For instance, Viessmann *et al.* [95] used harmonic imaging to highlight microbubbles in their channels. A similar harmonic technique was also used by O'Reilly and Hynynen [96]. Couture *et al.* [83] initially exploited slow-time filtering on large stacks of ultrafast images to highlight disruption or motion of the microbubbles. This approach was improved by using SVD of ultrafast data introduced initially for Doppler imaging [21] and applied here for ULM [99]. Such spatiotemporal filters based on SVD of ultrafast data can surpass nonlinear sequences even in clinical settings for slowly moving microbubbles (minimum 2 mm/s microbubble velocity in [33]). Further development by Ghosh *et al.* [103] and Lin *et al.* [104] has shown that selecting a population of larger microbubbles improves the signal-to-noise ratio of individualized microbubbles. Finally, nonlocal means filtering was introduced by Song *et al.* [105].

The second question, and possibly the most important, is the separation of microbubbles from each other. Indeed, the echoes from two microbubbles that are closer than a few wavelengths in a specific image will interfere, making the corresponding centroids of each microbubble indistinguishable or shifted. Consequently, only a limited number of microbubbles can be detected in each image to avoid such overlapping. For instance, in our brain experiments, we tend to localize around 100 microbubbles per ultrafast image. This limit contributes to the fundamental tradeoff between the attained super-resolution and the acquisition time as the number of microbubble events determines the smallest vessels that can be reconstructed. Couture *et al.* [83] initially proposed slow-time filtering of ultrafast data to extract microbubbles based on their motion or disruption. This approach was further improved by using SVD [99]. It is used to separate microbubbles from the surrounding tissue, the choice of the singular value threshold leading to an efficient extraction of microbubbles from tissue signature to the price of the exclusion of microbubbles that are too close from each other's. In London [95], [106], low concentrations of microbubbles were injected to guarantee that the echoes of multiple agents would not interfere. Such a solution, leading to longer acquisitions times or lower number of detected microbubbles was also preferred in Toronto by O'Reilly *et al.* and Hynynen [96]. However, their acquisition system relied on passive beamforming methods with a maximum attainable frame rate of 2 kHz at their imaging depth.

Along with the separation of microbubbles from tissue (CTR) and the separation of microbubbles from each other, the signal-to-noise ratio of an individual microbubble is a key element. Indeed, the resolution of an ULM image is determined by the localization precision of independent microbubbles. On the RF channel data, the microbubble echo appears, in time, as a hyperbola. The contrast for the detection of each pulse with respect of noise and tissue determines how accurately the fitting procedures can be applied on the maxima of the envelope or on the zero-crossing on each echo. In the end, it determines the maximum resolution of ULM. Because the beamformed data are often more readily available, a centroid detection procedure is applied, relying on local maxima search, convolution, or weighted-average approaches as in PALM [107].

Christensen-Jeffries *et al.* [108] demonstrated *in vitro* that the delayed response of the microbubbles had to be taken into account when localizing microbubbles. Indeed, because of their resonant nature, microbubbles do not scatter identically to the initial emitted pulse and tend to ring for a long period with respect to tissue. They proposed to use the signal onset as a reference because the exploitation of a Gaussian fitting method could lead to hundreds of micrometers in error. This is particularly important in the resonant regime of the contrast agent.

Since the super-resolved ULM images are reconstructed point by point, their resolution is preconditioned by the total number of microbubbles detected. Here, the distinction between the localization precision, introduced above, and the separability of the observable features is essential. Indeed, a blood vessel cannot be reconstructed with a single microbubble detection, even with a 1-picometers localization precision. A vessel needs several microbubble events to be reconstructed, and this number increases with the number of super-resolved pixels it encompasses. Smaller pixels require more microbubble events. For instance, in Errico *et al.* [99], the image was formed with close to 10-million super-resolved pixels. Considering that vessels are present in a great number of these pixels and that microbubble events are often superfluous in the same pixel, it took more than one million microbubble events to reconstruct a single image. Moreover,

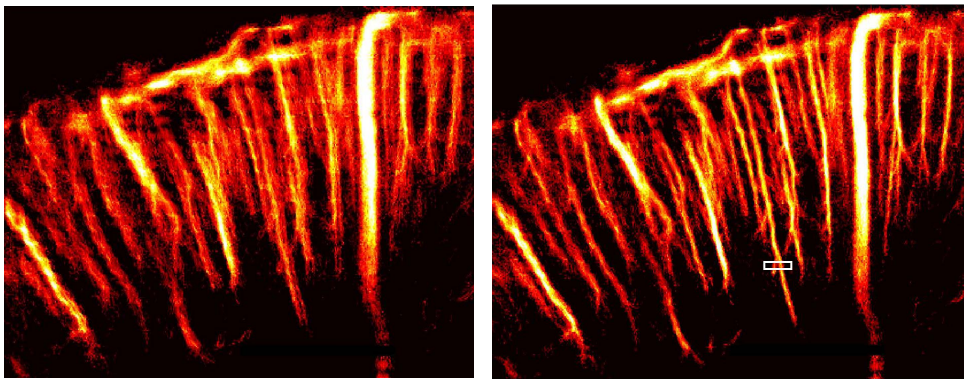

Fig. 5. ULM of the rat brain without (left) and with motion correction (right) based on phase-correlation of the ultrafast images (reproduced from [116] by permission of Elsevier, all rights reserved).

one should bear in mind vascular physiology as smaller vessels need much more time to be filled with microbubbles [109] and, irrespective of the localization method, should require longer acquisition time to be reconstructed [1], [110]. In the end, rather than the localization precision, the capacity of the imaging system to distinguish blood vessels much smaller than the wavelength represents a better measurement for resolution.

Because a single microbubble can reconstruct several pixels through its tracking during displacement trajectories, ultrasound microbubble tracking is a technique that can vastly improve the quality of images and modify its visualization. It was used initially in Errico *et al.* [99] and in Christensen-Jeffries *et al.* [106] to determine the velocity vector of individual microbubbles. Microbubbles flowing in blood vessels follow a smooth continuous track which can be reconstructed from a selected number of samples in the slow time. These samples are the localization of an individual microbubble in each image. The most basic algorithm of tracking is the closest-neighbor detector where a track is constructed iteratively by searching for the closest microbubble in the next image. A series of parameters is important such as the maximum distance a microbubble can propagate between two images, the intensity threshold to include or exclude the next microbubble, the criteria to initiate, and the criteria to terminate a track. More refined tracking algorithms were introduced such as Markov chain combined with Monte Carlo approaches [111], [112] or involving Hungarian assignment [105], [113]. The Hungarian assignment resolution implies linear operations on the cost matrix of the problem to solve the assignment problem of dimension n with an order of n^3 time complexity instead of an order of $n!$ time complexity with a conventional brute-force approach. As the number of particles is large in high-frame-rate acquisitions, this method is particularly efficient to assign the particles together. It was extensively used in transportation analysis [114].

As in pulsed Doppler, the sampling rate necessary to reconstruct a track depends on the velocity of the microbubble. Higher velocity should require higher frame rate. For slow flow, higher number of samples improves the tracking, as it simply adds more point to the curve fitting. However, the required sampling rate depends additionally on the distance between different microbubbles and the tracking algorithm. In other words, when comparing two successive ultrasonic images, can the ambiguity between a single and fast moving bubble, and two distinct bubbles be solved? Distinguishing the path of two neighboring microbubbles is made easier when the respective tracks are appropriately sampled in time. In our view, this is an important argument in favor of ultrafast imaging for ultrasound localization in addition to the improved speckle denoising.

Tracking is also a filter that can distinguish microbubbles from noise. Indeed, electronic noise does not follow a traceable path. Isolated points or very short tracks can be excluded from the image to improve the contrast between vessels and the surrounding bubble-less extravascular space.

Nevertheless, the main contribution of tracking is the possibility to create velocity maps. By determining the displacement of a microbubble between two images, a velocity vector can be created with a high dynamic range. Indeed, a millisecond sampling of a motion with a spatial resolution of 10 μm can yield velocities in the range of 0.1–10 mm/s and even more if the microbubbles are sparse. Moreover, the tracking in ultrasound localization imaging has much smaller dependence on direction than Doppler, which dominantly highlights axial displacements.

One of the strengths of ultrasound imaging is its temporal resolution which makes it such that motion can be exploited by the radiologists to assess the function of an organ such as the heart. However, motion is also a source of artifacts, particularly in ULM which requires long acquisitions to observe minute vessels. These vessels can be much smaller than the average displacements during a handheld scan. Several techniques have been used to reduce motion in the context of super-resolution. Christensen-Jeffries *et al.* [106] clamped a mouse ear with. Errico *et al.* [99] used a stereotactic frame to stabilize the brain. Lin *et al.* [115] excluded images where excessive motion due to breathing was present.

Motion can also be partly corrected using the cineloop where microbubbles are detected. Indeed, the phase dependence of ultrasound echoes opens the possibility to use precise subwavelength motion detection algorithms, much-like interferometry in optics. For instance, in shear wave elastography, micrometric displacement can be detected in the B-mode images even though the compression waves have wavelength hundreds of times larger. For ULM, Hingot *et al.* [116] (Fig. 5) gave a proof of concept using a very simple

speckle tracking approach based on phase-correlation between successive ultrafast images to correct for planar motion. Such a method could correct motion in the hundreds of micrometers in both directions in a brain without strict mechanical stabilization. However, the main contribution of this paper was the demonstration that the microbubble signal had to be removed from the images before motion correction as they can create false displacements by tens of micrometers. Similarly, Foiret *et al.* [117] have implemented their motion correction from the B-mode images while extracting their microbubbles from contrast pulse sequence (CPS). They were able to achieve correction of the kidney motion by several hundred micrometers in a free-breathing rat, adding a rotational component to the algorithm. Song *et al.* [105] also exploited phase-correlation rigid motion correction to align the kidney images in a free-breathing rabbit. Unfortunately, out-of-plane motions remain impossible to correct appropriately as the information is absent. Further development in 3-D ULM will become essential for the generalization of this technique.

A very important debate in the ULM community is the frame rate necessary to create super-resolved images. Indeed, subwavelength resolutions were obtained both with ultrafast frame rates (500 Hz and up [83], [97], [99], [115]–[117]) and conventional frame rates (around 30Hz [95], [96], [106], [111], [112], [118], [119]). Is ultrafast imaging at kilohertz frame rates really necessary for ULM? Especially since most available clinical scanners have yet to attain high frame rates, reducing the potential impact of the method in patient imaging. Opacic *et al.* [111] propose to exploit ULM tracking at conventional frame rates to reconstruct super-resolved vessels. Not only were they able to track microbubbles in vessels with a short acquisitions of 40 s (2000 images), but they were also able to extract parameters such as median distance between vessels, flow direction entropy, and other parameters that appear to change between tumor types *in vivo*. These parameters could become very relevant in cancer diagnosis. Discussions following the presentation of these results included the claim that ultrafast imaging could oversample the problem in time and that slow moving microbubbles do not need to be localized more than few tens of time per second if tracking is properly implemented. In our view, the question comes back to the definition of resolution, which is not the precision of localization of a single microbubble, but rather the separability of the microscopic features in an organ. According to the precision of localization, single tracks can be precise at the micrometer level. However, if only a very small fraction of microvessels are reconstructed at the smallest scale, then the image does not accurately depict the real vasculature. In some applications, a small sample of the microvasculature might be all it takes for diagnostically relevant information to be obtained, but in other applications a large fraction of the vessels will need to be reconstructed. In the latter case, millions of microbubble events are necessary and ultrafast imaging is likely to be required if experimentalists wish to be home for dinner.

In the end, many of these acoustical parameters depend strongly on the ultrasonic system, clinical or research, and on the ultrasonic probe. In most embodiments, linear arrays at various frequencies were exploited to perform ultrasound localization. However, O'Reilly and Hynynen [96] conceived their super-resolution experiment with a hemispherical 3-D ultrasonic array to reconstruct the microbubble position in 3-D. Desailly *et al.* [97] used parallel probes to achieve super-resolution in lateral, axial, and the elevation direction. Christensen-Jeffries *et al.* [108] rather proposed for the probes to be placed perpendicularly to attain an isotropic resolution in the three dimensions. Nevertheless, this method restricted the field of view to the confocal line between the two planes.

Through these technological developments, a series of new tradeoffs was discovered in ULM which went beyond the classical resolution versus penetration conundrum. Spatial resolution has been increased by almost two orders of magnitude, but it now depends on the time-resolution, number of microbubbles, signal-to-noise-ratio, tracking algorithm, probe geometry, vessel size, and many more parameters. These various parameters, shown in Table I, should therefore be described in the future publications for each tradeoff to be appropriately compared. Moreover, endpoint results such as localization precision and separability should be stated. These parameters will drastically affect the use of ULM in its preclinical and clinical applications.

TABLE I

PARAMETERS AFFECTING THE RESOLUTION OF ULM. IN OUR OPINION, THESE PARAMETERS AND ENDPOINTS SHOULD BE CLEARLY DISPLAYED IN FURTHER PUBLICATIONS BOTH *In Vitro* AND *In Vivo* TO GUARANTEE PROPER COMPARISONS

Important parameters
Signal-to-noise ratio
Contrast-to-tissue ratio
Contrast mechanism (linear / nonlinear)
Frame rate
Number of frame
Temporal jitter between electronic channels
Concentration of microbubbles
Infusion / bolus
Bubble-to-bubble separation approach
Frequency
Acquisition time
Number of microbubbles
Tracking algorithm
Track length
Data load
Perfusion characteristics of the organ (vessel density, blood flow)
Endpoints:
Localization precision of individual microbubbles
Detectability of subwavelength structures
Separability of subwavelength features
Statistics concerning velocity profiles

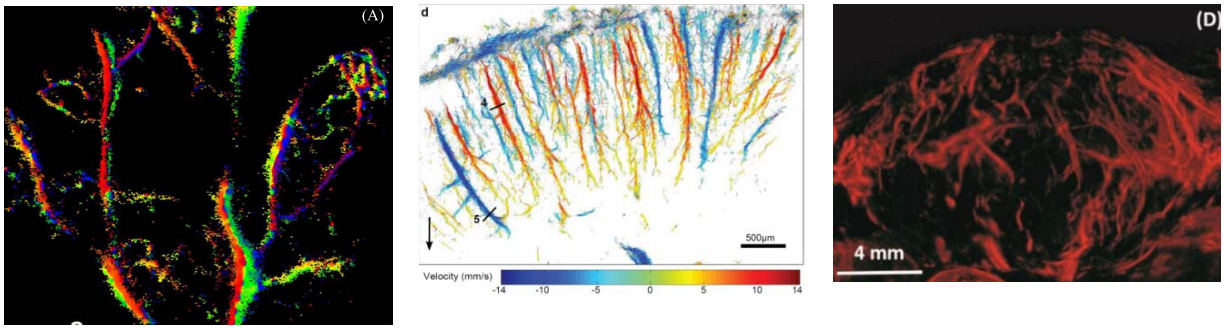

Fig. 6. Initial *in vivo* studies in ULM. Left: Mouse ear (© 2015 IEEE. Reprinted, with permission, from [106]). Center: Rat brain [99]. Right: Implanted tumor [115].

VI. Ultrasonic SOFI

SOFI is not a localization technique per se, as it rather exploits the stochastic fluctuations in subwavelength pixels to reduce the size of the point-spread function. However, as in ULM, its adaptation for ultrasound by the Technion Group [94], [120] exploits ultrafast imaging and microbubbles to improve resolution and it should be described in this review. In optics, SOFI uses smaller image stacks than other super-resolution techniques such as FPALM and STED since it does not require the localization of individual emitters [77]. Instead, it exploits the fact that the point-spread function of the images can be reduced by the properties of the cumulants in the slow-time direction. Indeed, the PSF is reduced by the square root of the order of the cumulant used. Although emitters are not localized, the technique still requires that some sources cycle between two distinguishable states. However, this process rapidly introduces noise artifacts and is usually restricted to lower order cumulants, leading to an improvement of resolution limited to a typical factor of 2. It is drastically lower than the improvement by FPALM, but it is faster by orders of magnitude and generally reduces the total fluence which damages cells in optical microscopy.

The approach taken by Bar-Zion *et al.* [94] is very similar to SOFI. In one study, they performed ultrafast imaging on VX-2 tumor xenograph in white rabbit model while injecting microbubbles. Various cumulants of the image stacks were exploited to recreate images showing some improvements in the vessel details. With a factor of 2 gain with respect to the resolution limit of the system for a 1000-frame acquisition, the results appear close to the images obtained without contrast agents using ultrafast Doppler and an inverse filter [121]. A more freshly fished approach based on SOFI in the case of sparse acquisitions, called SUSHI, was also proposed recently [122]. It was recently applied for the microvasculature imaging of the human prostate.

As SOFI is based on second-order statistics fluctuations rather than localization, it does not allow microscopic resolutions and should be compared in our opinion with concurrent approaches used in clinics, such as ultrafast power Doppler imaging [21] or superb microvascular imaging [123] rather than with localization microscopy.

VII. In Vivo Applications of Ultrasound Localization Microscopy

The deconvolution of single events corresponding to individual microbubbles were described in conventional [98] and ultrafast [83] imaging of murine tumor models. However, we would have to wait until 2015 for a proper subwavelength reconstruction of *in vivo* vasculature to be performed by two independent teams. The work of Christensen-Jeffries *et al.* [106] pursued the initial quest of their group to exploit a conventional scanner and low concentration of microbubbles to reveal the microvasculature of the mouse ear (Fig. 6(a)). They showed that they could visualize vessels down to 20 μm and confirmed their measurements with optical imaging of the same vessels. Although the total acquisition time was difficult to assess from this paper, with a frame rate of 25 Hz, the maximum injected volume of 200 μL at their maximum infusion rate could be reached between 40 and 1000 min, an acquisition time difficult to sustain from practical clinical applications.

In parallel, Errico *et al.* [99] also pursued their initial idea to exploit ultrafast differential imaging for ULM to explore the rat brain with a resolution of 8 μm [Fig. 6(b)]. The acquisition was done in 3 min with a single bolus for each plane, and several millions microbubble events were highlighted. This resolution of 8 μm was measured through statistical separability of the smallest pixels achievable with velocity tracking. Indeed, both groups [99], [106] introduced tracking of individual microbubbles to improve super-resolution imaging. This has become an essential component of super-resolution as it provides velocity measurements of individual microbubbles through time. The localization being done in the micrometer spatial resolution and millisecond timescale in the case of ultrafast ULM, the precision on the velocity vector is very high and Errico *et al.* [99] achieved a flow velocity dynamic range from less than 1 mm/s to several cm/s. Further studies on the brain [1] have confirmed that the maximum resolution is dependent on the number of microbubbles that are observed. The smallest vessels, such as capillaries, being only sparsely populated with microbubbles, the acquisition time increases when the super-resolved pixels and the vessels get smaller. Even though detecting a vessel of 100 μm can be performed in the hundreds of milliseconds, vessels of 5 μm in diameter takes several minutes to be described in their majority. In fact, in many applications where time resolution is more

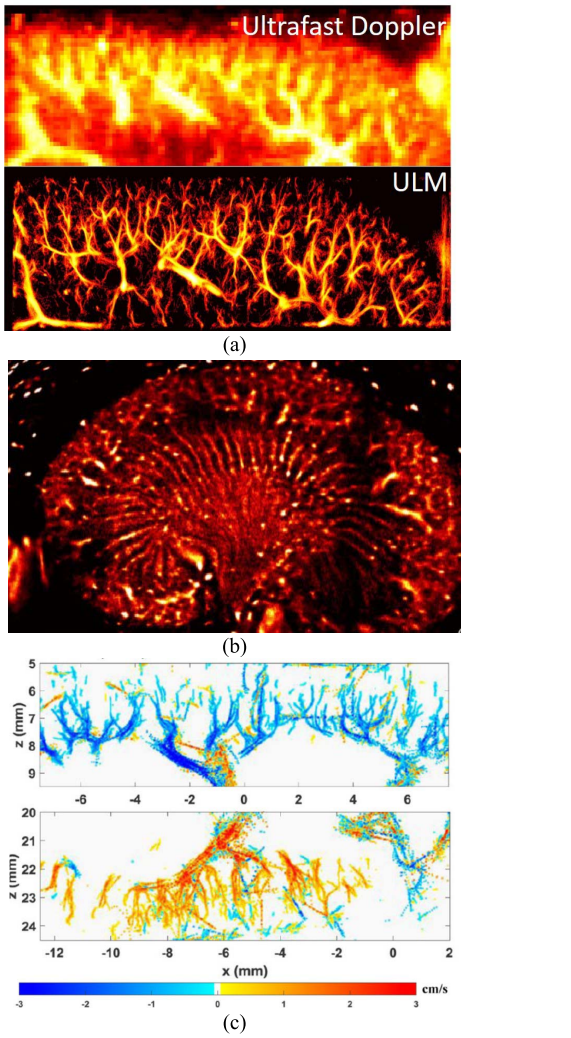

Fig. 7. (a) Ultrafast Doppler (top) and ultrafast ULM of the rat renal cortex (bottom). (b) ULM of the rat kidney from [117] (cropped from original under Creative Commons Attribution 4.0 International License). (c) ULM of rabbit kidney from [105] (© 2017 IEEE. Reprinted, with permission, from Song *et al.* 2018).

important than spatial resolution, ultrafast Doppler imaging [20] may remain a better approach for microvascular imaging [Fig. 7(a)] as it does not require microbubbles. Microbubbles will remain important when perfusion down to the capillary level is needed. In any case, ultrafast Doppler should always be performed on the same data set in comparison.

For practical clinical use, ULM should move beyond a simple description of the morphology of the microvasculature and allow the extraction of relevant biomarkers. Recent advances in the field are opening such applications. For instance, Lin *et al.* [115] [Fig. 6(c)] described the microvessels in subcutaneous tumor in rats by performing ultrafast ULM over several planes. The vessels were between 25 and 175 μm (wavelength = 330 μm). Moreover, the authors also described the tortuosity of the vessels at the microscopic scale and they showed an elevation in the tumor with respect to normal tissue. This is the first step in the direct description of the effect of angiogenesis on the conformation of microvessels for which ultrasound only provided indirect measurements until today, through reperfusion enhancement [124].

Opacic *et al.* [111], exploiting ULM tracking at conventional frame rates, also established new parameters for tumor characterization through microvessel imaging. They compared three different tumor types in mice, which were expected to display a diversity of vascular density (A431, MLS, and A546). They showed that they could extract biomarkers such as flow direction entropy and distances to the closest vessel, which differed in a statistically significant fashion between different tumor types.

Ghosh *et al.* [125] described the use of ULM with a clinical ultrasound scanner to monitor the effect of an angiogenesis inhibiting drug. They showed that the detected microvasculature was reduced by up to 60% within 2 h after the injection of Avastin versus 26% in the control tumor (likely due to experimental conditions). The same group [126] also described the use of ULM techniques to map the microvasculature in skeletal muscle of diabetic mice. Using various parameters, such as peak microbubble count, they showed the impaired microvascular response of obese animals to insulin, showing the potential of ULM to assess peripheral vascular damages in type-2 diabetes.

Foiret *et al.* [117] depicted the microvasculature of the rat kidney with ultrafast CPS mode. Nonlinear sequences and plane-wave imaging for microbubbles detection are far from being contradictory. It was even demonstrated that, at appropriate depth, it has higher CTR and lower disruption than nonlinear sequences at conventional frame rates [29], [30]. Beyond describing the microvascular anatomy of the kidney, Foiret *et al.* [117] also suggested that microbubbles which were constrained in small vessels would have longer persistence.

Finally, Luke *et al.* [127] have proposed to generalize ULM to vaporized nanodroplets. They showed the laser vaporization and the localization of the resulting microbubbles in the mouse brain. Acoustic droplet vaporization could probably also be used [128], [129]. In general, these nanodroplets tend to last longer and also penetrate tumors through the enhanced permeation and retention effect. Consequently, biological mechanisms other than intravascular flow could be explored through ULM.

These various applications of ULM, in the brain [99], in superficial vessels [106], in tumors [115], [125], in the kidney [117], are still at their infancy but show a pivotal evolution of the field. Indeed, initially, microvessels were used to demonstrate ULM as an imaging technique and displayed the anatomy of the microvasculature. More recent studies are showing that ULM can be used to extract useful information from these images such as the tortuosity of vessels, their mutual distances, or the stability of microbubbles in small vessels. Considering the evolution within the last seven years since its introduction, it probably has many tricks still to show.

VIII. Perspectives

With many independent groups working on the subject and energetic exchanges in international ultrasonic symposia, ULM is gaining momentum in research. In our view, there are still many developments and major discoveries to come.

The technological development is still a dynamic aspect of the field. Fundamental limits can be expanded by improving the separation of microbubbles from tissue and from each other's. Indeed, the localization precision determines the ultimate attainable resolution. Improving SNR and CTR can both contribute in bettering the precision below a few micrometers as most authors currently describe the limit to be. However, as microbubbles are purely intravascular, a resolution in the nanometer range might not be particularly relevant for most applications. Nevertheless, it can be used for new approaches such as physically distinguishing bound microbubbles from flowing microbubbles. In fact, one should envision ULM as deep microscopy and many applications currently limited to confocal or two-photon microscopy are now opened to ultrasound. It would vastly improve molecular imaging and allow the description of many new biological parameters at the micrometer scale.

One of the proximal goals for the field of ultrasound localization would be the validation of its accuracy. To date, *in vitro* demonstrations were concerned with precision, or the reproducibility of the localization within a confined vessel. *In vivo*, the quality of the super-resolved images is often evaluated through the self-coherence of the vessel branching pattern. In limited cases, a direct optical confirmation was possible [106] or the resolution was directly obtained from statistical variance of the measured blood velocity between subpixels [99]. But to establish the accuracy of ULM, it is necessary to compare it to established microscopy techniques such as confocal or two-photon microscopy.

The physics of microbubble oscillation has been a major subject of study in the last 20 years [130]. Currently, the localization of microbubble centroids remains very simplistic in this regard. Only Christensen-Jeffries *et al.* [108] have taken into account the resonant phenomena linked to microbubbles. Resonance, nonlinearities, disruption, and dedicated sequences should be used to improve the localization process. Using microbubble physics, ULM could even be used to probe the surrounding medium as it was suggested briefly by Foiret *et al.* [117]. Indeed, the localization of individual microbubbles could be used as an equivalent of an atomic force microscope *in vivo*. For instance, the micrometric motion induced by radiation force or other forces could be measured to assess the vessel elasticity or other mechanisms [131].

Beyond punctual localization, microbubble tracking should be the target of additional developments. Tracking improves drastically the images, under the condition that single microbubbles can be identified appropriately on each passing frame. Currently, this depends on the frame rate, the microbubble concentration, and the tracking algorithm. The latter can benefit from the all the developments in optical tracking and artificial intelligence. If a person can be followed in a crowd through video cameras, so should microbubbles in an organ! However, we have to keep in mind that the concentration of microbubbles cannot be increased indefinitely as very close microbubbles affect not only the tracking specificity, but also the localization process itself.

The requirement for tracking also imposes a general reduction in acoustic pressure to allow for microbubbles to remain intact over hundreds of images. In general, because of the exploitation of nonlinear sequences, microbubbles are used in a pressure range between the linear regime and the disruption regime. The disruption regime is stochastic; some microbubbles can disrupt after hundreds of pulses at a pressure deemed below the disruption threshold. For instance, we previously observed loss of 25% of the microbubble signal after 100 plane-wave images at 40-kPa peak-negative pressure at 7.5 MHz [30]. It is thus necessary to reduce imaging pressure to obtain long tracks, which excludes the use of several nonlinear sequences. Further improvements in linear detection of microbubbles might be important [33].

ULM with other agents than microbubbles could open avenues other than microvascular imaging. Indeed, the localization of the vaporization of droplets [129] would allow for the observation of extravascular contrast agents, accumulated, for example, by the enhanced-permeability and retention effect. ULM could map the interstitial environment and even determine the intratumoral conditions through the slow displacement of resulting microbubbles. The exhilarating development of ultrasonic reporter genes [132] could also be applied in ULM. Rather than tracking microbubbles, it would be possible to track cells that express the genes for the production of nanovesicles.

But, one of the main developments in ULM will probably be its generalization to 3-D imaging using 2-D arrays. Indeed, we are facing many limitations linked to planar imaging. First, there is a clear asymmetry between the few micrometer resolutions; we can obtain in the axial–lateral plane versus the elevation resolution limited by diffraction from a physical lense on the probe. Consequently, vessels in the elevation are projected in the plane and can be blurred. Moreover, the plane thickness is difficult to determine precisely, as an off-plane but highly scattering microbubble could appear as an in-plane poorly scattering object. Tracking is also not possible in the third dimension. Moreover, ULM is very sensitive to motion and its correction cannot be obtained in a direction without spatial sampling. Finally, plane-by-plane super-resolution is impractical due to the acquisition time of each plane which corresponds to the duration of the injected bolus (few minutes). Currently, multiple boluses or constant infusion is thus necessary to have a pseudo-3-D super-resolved ultrasound image. Early work on 3-D super-resolution imaging [96], [97] has attempted to solve these various issues, but we are still waiting for the entire characterization of an organ with volumetric ultrasound super-resolution. The 3-D imaging will allow for an isotropic super-resolution, with isotropic motion correction and a complete characterization of vectorial flow. Moreover, we should be able to obtain a full volume in a time similar to that of a single plane in the current situation. Indeed, a 2-D array should be capable of distinguishing many more microbubbles per acquired volume than a 1-D array can detect in a single image. Obviously, 3-D ULM will create massive amount of data, but Moore's law should take care of this limitation in due time. Moreover, localization is the ultimate

data compression tool as a Gigabit-sized stack of frames can be compacted into a kilobit-sized list of microbubble positions and timing.

Beyond technological advances, many new applications of ULM are likely to appear in the near future; both in animals for model characterization and in human for diagnosis and monitoring. One of the conclusions of the work of Lin *et al.* [115] and Opacic *et al.* [111] is that ULM provides direct access to quantifiable microvascular parameters, which were only accessible indirectly in the past through reperfusion imaging. In fact, ULM might even replace disruption-reperfusion imaging as it provides more detailed information on the microvasculature. The vascular organization of tumors might give a clear contrast with surrounding healthy tissue, especially in highly organized organs such as the kidney, the liver, and the brain. With appropriate motion correction and 3-D imaging, the heart could even become accessible to ULM, providing a new characterization for coronary arteries.

In general, ULM is less a microvascular imaging method, than a technique to challenge the compromise between resolution and penetration. In many situations, the observation of capillaries or microarterioles should not be necessary. It suffices to breach a resolution limit imposed by the depth of an organ or the presence of a bone interface to yield interesting new information. For instance, deep-seated tumor in the liver could be explored at a resolution below 100 μm with a conventional bolus of microbubbles (several hundred millions). However, it might be necessary to combine motion tracking and breath holding. In transcranial imaging, the resolution could no longer be limited to about 1 mm, which is defined by the low frequencies ($<$2 MHz) that can penetrate the skull.

In the brain, ULM could also be combined with blood-brain barrier opening [133] to yield a better localization of the vascular effect of the microbubble oscillation. Indeed, the effective microbubbles could be imaged while they induce a mechanical stress on the vascular wall. The same approach would also help the characterization and the mapping of the sonoporation effect [134]. In fact, ULM could become a key aspect of theranostics for monitoring. Recent advances have demonstrated that ultrasonic therapy itself could be performed with a subwavelength resolution [129].

Finally, the future of ULM is linked to its various *in vivo* applications and manufacturers of clinical scanners should be associated for further developments. ULM opens a new window on microvasculature which could not be observed before because it was either too small or too deep. Considering that most of the main killers involve the smallest blood vessels (cardiovascular diseases, stroke, cancer, diabetes), there should be no lack of applications.

IX. Conclusion

ULM is the younger cousin of optical localization microscopy. While the latter has been crowned with success in laboratories, the former remains in its infancy but shows an enormous potential for clinical applications. ULM already demonstrated some technical prowess, such as the visualization of the microvasculature, in depth, at a resolution which is a 10th of the wavelength of the ultrasound in the brain, in tumors and in the kidney. Various ongoing developments will extend its applicability to the microvasculature in all organs in animals, but especially in humans. ULM should become a diagnosis modality which will provide information on the biological processes at a micrometric scale deep within tissue.

Acknowledgment

The authors would like to thank J. Provost for fruitful discussions.

References

[1] V. Hingot, C. Errico, B. Heiles, L. Rahal, M. Tanter, and O. Couture, "Incompressible perfusion time of microbubbles drives the fundamental compromise between spatial resolution and acquisition time in ultrasound localization microscopy," *J. Cerebral Blood Flow Metabolism*, submitted for publication.

[2] C. Chilowsky and P. Langevin, "Procédés et appareils pour la production de signaux sous-marins dirigés et pour la localisation á distance d'obstacles sous-marins," French Patent 502.913, May 29, 1916.

[3] K. T. Dussik, "On the possibility of using ultrasound waves as a diagnostic aid," *Neurol. Psychiat*, vol. 174, pp. 153–168, 1942.

[4] P. G. Newman and G. S. Rozycki, "The history of ultrasound," *Surg. Clinics North Amer.*, vol. 78, no. 2, pp. 179–195, 1998.

[5] R. S. C. Cobbold, *Foundations of Biomedical Ultrasound*. London, U.K.: Oxford Univ. Press, 2007, pp. 45–51.

[6] R. Gramiak, P. M. Shah, and D. H. Kramer, "Ultrasound cardiography: Contrast studies in anatomy and function," *Radiology*, vol. 92, no. 5, pp. 939–948, 1969.

[7] T. Leighton, "The acoustic bubble," *World J. Urol.*, 1994.

[8] H. Mulvana *et al.*, "Characterization of contrast agent microbubbles for ultrasound imaging and therapy research," *IEEE Trans. Ultrason., Ferroelectr., Freq. Control*, vol. 64, no. 1, pp. 232–251, Jan. 2017.

[9] A. L. Klibanov *et al.*, "Detection of individual microbubbles of ultrasound contrast agents: Imaging of free-floating and targeted bubbles," *Invest. Radiol.*, vol. 39, no. 3, pp. 187–195, 2004.

[10] M. Brannigan, P. N. Burns, and S. R. Wilson, "Blood flow patterns in focal liver lesions at microbubble-enhanced U.S.," *Radiographics*, vol. 24, no. 4, pp. 35–921, 2004.

[11] H. Wijkstra, M. H. Wink, and J. J. M. C. H. de la Rosette, "Contrast specific imaging in the detection and localization of prostate cancer," *World J. Urol.*, vol. 22, no. 5, pp. 346–350, 2004.

[12] W. Lepper, T. Belcik, K. Wei, and J. Lindner, "Myocardial contrast echocardiography," *Circulation*, vol. 109, no. 25, pp. 3132–3135, 2004.

[13] M. Tanter and M. Fink, "Ultrafast imaging in biomedical ultrasound," *IEEE Trans. Ultrason., Ferroelectr., Freq. Control*, vol. 61, no. 1, pp. 102–119, Jan. 2014.

[14] C. Bruneel, R. Torguet, K. M. Rouvaen, E. Bridoux, and B. Nongaillard, "Ultrafast echotomographic system using optical processing of ultrasonic signals," *Appl. Phys. Lett.*, vol. 30, no. 8, pp. 371–373, 1977.

[15] B. Delannoy, R. Torguet, C. Bruneel, E. Bridoux, J. M. Rouvaen, and H. Lasota, "Acoustical image reconstruction in parallel-processing analog electronic systems," *J. Appl. Phys.*, vol. 50, no. 5, pp. 3153–3159, 1979.

[16] L. Sandrin, S. Catheline, M. Tanter, X. Hennequin, and M. Fink, "Time-resolved pulsed elastography with ultrafast ultrasonic imaging," *Ultrason. Imag.*, vol. 21, no. 4, pp. 259–272, Oct. 1999.

[17] M. Tanter, J. Bercoff, L. Sandrin, and M. Fink, "Ultrafast compound imaging for 2-D motion vector estimation: Application to transient elastography," *IEEE Trans. Ultrason., Ferroelectr., Freq. Control*, vol. 49, no. 10, pp. 1363–1374, Oct. 2002.

[18] M. Tanter *et al.*, "Quantitative assessment of breast lesion viscoelasticity: Initial clinical results using supersonic shear imaging," *Ultrasound Med. Biol.*, vol. 34, no. 9, pp. 1373–1386, Sep. 2008.

[19] É. Bavu, "Noninvasive *in vivo* liver fibrosis evaluation using supersonic shear imaging: A clinical study on 113 hepatitis C virus patients," *Ultrasound Med. Biol.*, vol. 37, no. 9, pp. 1361–1373, 2011.

[20] J. Bercoff *et al.*, "Ultrafast compound Doppler imaging: Providing full blood flow characterization," *IEEE Trans. Ultrason., Ferroelectr., Freq. Control*, vol. 58, no. 1, pp. 134–147, Jan. 2011.

[21] C. Demené *et al.*, "Spatiotemporal clutter filtering of ultrafast ultrasound data highly increases Doppler and fUltrasound sensitivity," *IEEE Trans. Med. Imag.*, vol. 34, no. 11, pp. 2271–2285, Nov. 2015.

[22] C. Demené *et al.*, "Ultrafast Doppler reveals the mapping of cerebral vascular resistivity in neonates," *J. Cerebral Blood Flow Metabolism*, vol. 34, no. 6, pp. 1009–1017, Jun. 2014.

[23] E. Macé, G. Montaldo, I. Cohen, M. Baulac, M. Fink, and M. Tanter, "Functional ultrasound imaging of the brain," *Nature Methods*, vol. 8, pp. 662–664, May 2011.

[24] T. Deffieux, C. Demene, M. Pernot, and M. Tanter, "Functional ultrasound neuroimaging: A review of the preclinical and clinical state of the art," *Current Opinion Neurol.*, vol. 50, pp. 128–135, Jun. 2018.

[25] L.-A. Sieu *et al.*, "EEG and functional ultrasound imaging in mobile rats," *Nature Methods*, vol. 12, no. 9, pp. 831–834, 2015.

[26] A. Urban, C. Dussaux, G. Martel, C. Brunner, E. Mace, and G. Montaldo, "Real-time imaging of brain activity in freely moving rats using functional ultrasound," *Nature Methods*, vol. 12, pp. 873–878, Sep. 2015.

[27] C. Demene *et al.*, "Functional ultrasound imaging of brain activity in human newborns," *Sci. Transl. Med.*, vol. 9, no. 411, pp. 1–11, 2017.

[28] M. Imbault, D. Chauvet, J.-L. Gennisson, L. Capelle, and M. Tanter, "Intraoperative functional ultrasound imaging of human brain activity," *Sci. Rep.*, vol. 7, Aug. 2017, Art. no. 7304.

[29] O. Couture, S. Bannouf, G. Montaldo, J. F. Aubry, M. Fink, and M. Tanter, "Ultrafast imaging of ultrasound contrast agents," *Ultrasound Med. Biol.*, vol. 35, no. 11, pp. 1908–1916, 2009.

[30] O. Couture, M. Fink, and M. Tanter, "Ultrasound contrast plane wave imaging," *IEEE Trans. Ultrason., Ferroelectr., Freq. Control*, vol. 59, no. 12, pp. 2676–2683, Dec. 2012.

[31] C. Tremblay-Darveau, R. Williams, L. Milot, M. Bruce, and P. N. Burns, "Combined perfusion and Doppler imaging using plane-wave nonlinear detection and microbubble contrast agents," *IEEE Trans. Ultrason., Ferroelectr., Freq. Control*, vol. 61, no. 12, pp. 1988–2000, Dec. 2014.

[32] C. Errico, B.-F. Osmanski, S. Pezet, O. Couture, Z. Lenkei, and M. Tanter, "Transcranial functional ultrasound imaging of the brain using microbubble-enhanced ultrasensitive Doppler," *NeuroImage*, vol. 124, pp. 752–761, Jan. 2016.

[33] Y. Desailly, A.-M. Tissier, J.-M. Correas, F. Wintzenrieth, M. Tanter, and O. Couture, "Contrast enhanced ultrasound by real-time spatiotemporal filtering of ultrafast images," *Phys. Med. Biol.*, vol. 62, no. 1, pp. 31–42, 2017.

[34] P. J. Kaczkowski and R. E. Daigle, "The Verasonics ultrasound system as a pedagogic tool in teaching wave propagation, scattering, beamforming, and signal processing concepts in physics and engineering," *J. Acoust. Soc. Amer.*, vol. 129, no. 4, p. 2648, 2011.

[35] P. Tortoli, L. Bassi, E. Boni, A. Dallai, F. Guidi, and S. Ricci, "ULA-OP: An advanced open platform for ultrasound research," *IEEE Trans. Ultrason., Ferroelectr., Freq. Control*, vol. 56, no. 10, pp. 2207–2216, Oct. 2009.

[36] M. Fink, G. Montaldo, and M. Tanter, "Time-reversal acoustics in biomedical engineering," *Annu. Rev. Biomed. Eng.*, vol. 5, pp. 465–497, Jun. 2003.

[37] F. Tranquart, N. Grenier, V. Eder, and L. Pourcelot, "Clinical use of ultrasound tissue harmonic imaging," *Ultrasound Med. Biol.*, vol. 25, no. 6, pp. 889–894, 1999.

[38] K. J. Parker, M. S. Asztely, R. M. Lerner, E. A. Schenk, and R. C. Waag, "*In-vivo* measurements of ultrasound attenuation in normal or diseased liver," *Ultrasound Med. Biol.*, vol. 14, no. 2, pp. 127–136, 1988.

[39] G. R. Lockwood, D. H. Turnball, D. A. Christopher, and F. S. Foster, "Beyond 30 MHz," *IEEE Eng. Med. Biol. Mag.*, vol. 15, no. 6, pp. 60–71, Nov./Dec. 1996.

[40] F. S. Foster *et al.*, "A new 15–50 MHz array-based micro-ultrasound scanner for preclinical imaging," *Ultrasound Med. Biol.*, vol. 35, no. 10, pp. 1700–1708, 2009.

[41] D. E. Goertz, J. L. Yu, R. S. Kerbel, P. N. Burns, and F. S. Foster, "High-frequency Doppler ultrasound monitors the effects of antivascular therapy on tumor blood flow," *Cancer Res.*, vol. 62, no. 22, pp. 6371–6375, 2002.

[42] L. Sun *et al.*, "A high-frame rate high-frequency ultrasonic system for cardiac imaging in mice," *IEEE Trans. Ultrason., Ferroelectr., Freq. Control*, vol. 54, no. 8, pp. 1648–1655, Aug. 2007.

[43] D. H. Turnbull and F. S. Foster, "*In vivo* ultrasound biomicroscopy in developmental biology," *Trends Biotechnol.*, vol. 20, no. 8, pp. S29–S33, 2002.

[44] B. J. Potkin *et al.*, "Coronary artery imaging with intravascular high-frequency ultrasound," *Circulation*, vol. 81, no. 5, pp. 1575–1585, 1990.

[45] R. C. Gessner, C. B. Frederick, F. S. Foster, and P. A. Dayton, "Acoustic angiography: A new imaging modality for assessing microvasculature architecture," *Int. J. Biomed. Imag.*, vol. 2013, Jun. 2013, Art. no. 936593.

[46] S. E. Shelton *et al.*, "Quantification of microvascular tortuosity during tumor evolution using acoustic angiography," *Ultrasound Med. Biol.*, vol. 41, no. 7, pp. 1896–1904, Jul. 2015.

[47] G. S. Shekhawat and V. P. Dravid, "Nanoscale imaging of buried structures via scanning near-field ultrasound holography," *Science*, vol. 310, no. 5745, pp. 89–92, 2005.

[48] M. Fink and M. Tanter, "Multiwave imaging and super resolution," *Phys. Today*, vol. 63, no. 2, pp. 28–33, 2010.

[49] G. Lerosey, J. de Rosny, A. Tourin, and M. Fink, "Focusing beyond the diffraction limit with far-field time reversal," *Science*, vol. 315, no. 5815, pp. 1120–1122, 2007.

[50] J. B. Pendry, "Negative refraction makes a perfect lens," *Phys. Rev. Lett.*, vol. 85, no. 18, pp. 3966–3969, Oct. 2000.

[51] J. H. Page, "Focusing of ultrasonic waves by negative refraction in phononic crystals," *AIP Adv.*, vol. 6, no. 12, p. 121606, 2016.

[52] M. Lanoy, R. Pierrat, F. Lemoult, M. Fink, V. Leroy, and A. Tourin, "Subwavelength focusing in bubbly media using broadband time reversal," *Phys. Rev. B, Condens. Matter*, vol. 91, no. 22, p. 224202, 2015.

[53] P. Blomgren, G. Papanicolaou, and H. Zhao, "Super-resolution in time-reversal acoustics," *J. Acoust. Soc. Amer.*, vol. 111, no. 1, pp. 230–248, 2002.

[54] S. K. Lehman and A. J. Devaney, "Transmission mode time-reversal super-resolution imaging," *J. Acoust. Soc. Amer.*, vol. 113, no. 5, pp. 2742–2753, 2003.

[55] C. Prada and J.-L. Thomas, "Experimental subwavelength localization of scatterers by decomposition of the time reversal operator interpreted as a covariance matrix," *J. Acoust. Soc. Amer.*, vol. 114, no. 1, pp. 235–243, 2003.

[56] G. T. Clement, J. Huttunen, and K. Hynynen, "Superresolution ultrasound imaging using back-projected reconstruction," *J. Acoust. Soc. Amer.*, vol. 118, no. 6, pp. 3953–3960, 2005.

[57] T. Ilovitsh, A. Ilovitsh, J. Foiret, B. Z. Fite, and K. W. Ferrara, "Acoustical structured illumination for super-resolution ultrasound imaging," *Commun. Biol.*, vol. 1, Jan. 2018, Art. no. 3.

[58] O. Ikeda, T. Sato, and K. Suzuki, "Super-resolution imaging system using waves with a limited frequency bandwidth," *J. Acoust. Soc. Amer.*, vol. 65, no. 1, pp. 75–81, 1979.

[59] H. W. Jones, "Superresolution in ultrasonic imaging," in *Acoustical Imaging*. Boston, MA, USA: Springer, 1992, pp. 71–76.

[60] E. Betzig and J. K. Trautman, "Near-field optics: Microscopy, spectroscopy, and surface modification beyond the diffraction limit," *Science*, vol. 257, no. 5067, pp. 189–195, 1992.

[61] D. Lu and Z. Liu, "Hyperlenses and metalenses for far-field super-resolution imaging," *Nature Commun.*, vol. 3, Nov. 2012, Art. no. 1205.

[62] M. G. L. Gustafsson, "Surpassing the lateral resolution limit by a factor of two using structured illumination microscopy," *J. Microsc.*, vol. 198, no. 2, pp. 7–82, 2000.

[63] E. Betzig *et al.*, "Imaging intracellular fluorescent proteins at nanometer resolution," *Science*, vol. 313, no. 5793, pp. 1642–1645, 2006.

[64] L. Möckl, D. C. Lamb, and C. Bräuchl, "Super-resolved fluorescence microscopy: Nobel prize in chemistry 2014 for Eric Betzig, Stefan Hell, and William E. Moerner," *Angew. Chemie Int. Ed.*, vol. 53, no. 51, pp. 13972–13977, 2014.

[65] S. Udenfriend, *Fluorescence Assay in Biology and Medicine*. New York, NY, USA: Academic, 1969.

[66] M. Chalfie, Y. Tu, G. Euskirchen, W. W. Ward, and D. C. Prasher, "Green fluorescent protein as a marker for gene expression," *Science*, vol. 263, no. 5148, pp. 802–805, 1994.

[67] W. E. Moerner and L. Kador, "Optical detection and spectroscopy of single molecules in a solid," *Phys. Rev. Lett.*, vol. 62, no. 21, pp. 2535–2538, 1989.

[68] E. Betzig and R. J. Chichester, "Single molecules observed by near-field scanning optical microscopy," *Science*, vol. 262, no. 5138, pp. 1422–1425, 1993.

[69] S. W. Hell and J. Wichmann, "Breaking the diffraction resolution limit by stimulated emission: Stimulated-emission-depletion fluorescence microscopy," *Opt. Lett.*, vol. 19, no. 11, pp. 780–782, 1994.

[70] S. W. Hell, "Far-field optical nanoscopy," *Science*, vol. 316, no. 5828, pp. 1153–1158, 2007.

[71] M. A. Lauterbach, C. K. Ullal, V. Westphal, and S. W. Hell, "Dynamic imaging of colloidal-crystal nanostructures at 200 frames per second," *Langmuir*, vol. 26, no. 18, pp. 14400–14404, 2010.

[72] S. T. Hess, T. P. K. Girirajan, and M. D. Mason, "Ultra-high resolution imaging by fluorescence photoactivation localization microscopy," *Biophys. J.*, vol. 91, no. 11, pp. 4258–4272, Dec. 2006.

[73] M. J. Rust, M. Bates, and X. Zhuang, "Sub-diffraction-limit imaging by stochastic optical reconstruction microscopy (STORM)," *Nature Methods*, vol. 3, no. 10, pp. 793–796, 2006.

[74] B. Huang, H. Babcock, and X. Zhuang, "Breaking the diffraction barrier: Super-resolution imaging of cells," *Cell*, vol. 143, no. 7, pp. 1047–1058, 2010.

[75] H. Deschout *et al.*, "Precisely and accurately localizing single emitters in fluorescence microscopy," *Nature Methods*, vol. 11, pp. 253–266, Feb. 2014.

[76] A. von Diezmann, Y. Shechtman, and W. E. Moerner, "Three-dimensional localization of single molecules for super-resolution imaging and single-particle tracking," *Chem. Rev.*, vol. 117, no. 11, pp. 7244–7275, 2017.

[77] T. Dertinger, R. Colyer, G. Iyer, S. Weiss, and J. Enderlein, "Fast, background-free, 3D super-resolution optical fluctuation imaging (SOFI)," *Proc. Nat. Acad. Sci. USA*, vol. 106, no. 52, pp. 22287–22292, Dec. 2009.

[78] S. Geissbuehler, C. Dellagiacoma, and T. Lasser, "Comparison between SOFI and STORM," *Biomed. Opt. Exp.*, vol. 2, no. 3, pp. 408–420, 2011.

[79] P. Sengupta, S. B. van Engelenburg, and J. Lippincott-Schwartz, "Superresolution imaging of biological systems using photoactivated localization microscopy," *Chem. Rev.*, vol. 114, no. 6, pp. 3189–3202, 2014.

[80] H. Shroff, C. G. Galbraith, J. A. Galbraith, and E. Betzig, "Live-cell photoactivated localization microscopy of nanoscale adhesion dynamics," *Nature Methods*, vol. 5, pp. 417–423, May 2008.

[81] S. Manley *et al.*, "High-density mapping of single-molecule trajectories with photoactivated localization microscopy," *Nature Methods*, vol. 5, no. 2, pp. 155–157, 2008.

[82] G. Shtengel *et al.*, "Interferometric fluorescent super-resolution microscopy resolves 3D cellular ultrastructure," *Proc. Nat. Acad. Sci. USA*, vol. 106, no. 9, pp. 3125–3130, 2009.

[83] O. Couture, B. Besson, G. Montaldo, M. Fink, and M. Tanter, "Microbubble ultrasound super-localization imaging (MUSLI)," in *Proc. IEEE Int. Ultrason. Symp. (IUS)*, Oct. 2011, pp. 1285–1287.

[84] O. Couture, M. Tanter, and M. Fink, "Method and device for ultrasound imaging," Patent Cooperation Treaty PCT/FR2011/052 810, 2011.

[85] J. Gateau, J.-F. Aubry, M. Pernot, M. Fink, and M. Tanter, "Combined passive detection and ultrafast active imaging of cavitation events induced by short pulses of high-intensity ultrasound," *IEEE Trans. Ultrason., Ferroelectr., Freq. Control*, vol. 58, no. 3, pp. 517–532, Mar. 2011.

[86] S. R. Wilson, L. D. Greenbaum, and B. B. Goldberg, "Contrast-enhanced ultrasound: What is the evidence and what are the obstacles?" *Amer. J. Roentgenol.*, vol. 193, no. 1, pp. 55–60, 2009.

[87] D. H. Evans and W. N. McDicken, *Doppler Ultrasound: Physics, Instrumentation and Signal Processing*. New York, NY, USA: Wiley, 2000.

[88] W. F. Walker and G. E. Trahey, "A fundamental limit on delay estimation using partially correlated speckle signals," *IEEE Trans. Ultrason., Ferroelectr., Freq. Control*, vol. 42, no. 2, pp. 301–308, Mar. 1995.

[89] J. Sun and K. Hynynen, "Focusing of therapeutic ultrasound through a human skull: A numerical study," *J. Acoust. Soc. Amer.*, vol. 104, no. 3, pp. 1705–1715, 1998.

[90] A. Tourin, A. Derode, and M. Fink, "Dynamic time reversal of randomly backscattered acoustic waves," *Europhys. Lett.*, vol. 47, no. 2, pp. 175–181, 1999.

[91] O. Couture, J. F. Aubry, G. Montaldo, M. Tanter, and M. Fink, "Suppression of tissue harmonics for pulse-inversion contrast imaging using time reversal," *Phys. Med. Biol.*, vol. 53, no. 19, pp. 5469–5480, 2008.

[92] G. Montaldo, M. Tanter, J. Bercoff, N. Benech, and M. Fink, "Coherent plane-wave compounding for very high frame rate ultrasonography and transient elastography," *IEEE Trans. Ultrason., Ferroelectr., Freq. Control*, vol. 56, no. 3, pp. 489–506, Mar. 2009.

[93] J. Provost *et al.*, "3D ultrafast ultrasound imaging *in vivo*," *Phys. Med. Biol.*, vol. 59, no. 19, pp. L1–L13, 2014.

[94] A. Bar-Zion, C. Tremblay-Darveau, O. Solomon, D. Adam, and Y. C. Eldar, "Fast vascular ultrasound imaging with enhanced spatial resolution and background rejection," *IEEE Trans. Med. Imag.*, vol. 36, no. 1, pp. 169–180, Jan. 2017.

[95] O. M. Viessmann, R. J. Eckersley, K. Christensen-Jeffries, M. X. Tang, and C. Dunsby, "Acoustic super-resolution with ultrasound and microbubbles," *Phys. Med. Biol.*, vol. 58, no. 18, pp. 6447–6458, Sep. 2013.

[96] M. A. O'Reilly and K. Hynynen, "A super-resolution ultrasound method for brain vascular mapping," *Med. Phys.*, vol. 40, no. 11, p. 110701, 2013.

[97] Y. Desailly, O. Couture, M. Fink, and M. Tanter, "Sono-activated ultrasound localization microscopy," *Appl. Phys. Lett.*, vol. 103, no. 17, p. 174107, 2013.

[98] M. Siepmann, G. Schmitz, J. Bzyl, M. Palmowski, and F. Kiessling, "Imaging tumor vascularity by tracing single microbubbles," in *Proc. IEEE Int. Ultrason. Symp. (IUS)*, Oct. 2011, pp. 1906–1908.

[99] C. Errico *et al.*, "Ultrafast ultrasound localization microscopy for deep super-resolution vascular imaging," *Nature*, vol. 527, no. 7579, pp. 499–502, Nov. 2015.

[100] Y. Desailly, J. Pierre, O. Couture, and M. Tanter, "Resolution limits of ultrafast ultrasound localization microscopy," *Phys. Med. Biol.*, vol. 60, no. 22, pp. 8723–8740, Nov. 2015.

[101] P. Song, A. Manduca, J. D. Trzasko, R. E. Daigle, and S. Chen, "Sampling quantization in super-resolution ultrasound microvessel imaging," *IEEE Trans. Ultrason., Ferroelectr., Freq. Control*, to be published.

[102] P. N. Burns and S. R. Wilson, "Microbubble contrast for radiological imaging: 1. Principles," *Ultrasound Quart.*, vol. 22, no. 1, pp. 5–13, 2006.

[103] D. Ghosh, F. Xiong, S. R. Sirsi, P. W. Shaul, R. F. Mattrey, and K. Hoyt, "Toward optimization of *in vivo* super-resolution ultrasound imaging using size-selected microbubble contrast agents," *Med. Phys.*, vol. 44, no. 12, pp. 6304–6313, 2017.

[104] F. Lin, J. K. Tsuruta, J. D. Rojas, and P. A. Dayton, "Optimizing sensitivity of ultrasound contrast-enhanced super-resolution imaging by tailoring size distribution of microbubble contrast agent," *Ultrasound Med. Biol.*, vol. 43, no. 10, pp. 2488–2493, 2017.

[105] P. Song *et al.*, "Improved super-resolution ultrasound microvessel imaging with spatiotemporal nonlocal means filtering and bipartite graph-based microbubble tracking," *IEEE Trans. Ultrason., Ferroelectr., Freq. Control*, vol. 65, no. 2, pp. 149–167, Feb. 2018.

[106] K. Christensen-Jeffries, R. J. Browning, M.-X. Tang, C. Dunsby, and R. J. Eckersley, "*In vivo* acoustic super-resolution and super-resolved velocity mapping using microbubbles," *IEEE Trans. Med. Imag.*, vol. 34, no. 2, pp. 433–440, Feb. 2015.

[107] R. Henriques, M. Lelek, E. F. Fornasiero, F. Valtorta, C. Zimmer, and M. M. Mhlanga, "QuickPALM: 3D real-time photoactivation nanoscopy image processing in ImageJ," *Nature Methods*, vol. 7, no. 5, pp. 339–340, 2010.

[108] K. Christensen-Jeffries *et al.*, "Microbubble axial localization errors in ultrasound super-resolution imaging," *IEEE Trans. Ultrason., Ferroelectr., Freq. Control*, vol. 64, no. 11, pp. 1644–1654, Nov. 2017.

[109] F. W. Prinzen and J. B. Bassingthwaighte, "Blood flow distributions by microsphere deposition methods," *Cardiovascular Res.*, vol. 45, no. 1, pp. 13–21, 2000.

[110] S. Dencks, M. Piepenbrock, G. Schmitz, T. Opacic, and F. Kiessling, "Determination of adequate measurement times for super-resolution characterization of tumor vascularization," in *Proc. IEEE Int. Ultrason. Symp. (IUS)*, Sep. 2017, pp. 1–4.

[111] T. Opacic *et al.*, "Super-resolution ultrasound bubble tracking for pre-clinical and clinical multiparametric tumor characterization," *bioRxiv*, p. 203935, 2017.

[112] D. Ackermann, G. Schmitz, and S. Member, "Detection and tracking of multiple microbubbles in ultrasound B-mode images," *IEEE Trans. Ultrason., Ferroelectr., Freq. Control*, vol. 63, no. 1, pp. 72–82, Jan. 2016.

[113] H. W. Kuhn, "The Hungarian method for the assignment problem," *Naval Res. Logistics Quart.*, vol. 2, nos. 1–2, pp. 83–97, Mar. 1955.

[114] J. Munkres, "Algorithms for the assignment and transportation problems," *J. Soc. Ind. Appl. Math.*, vol. 5, no. 1, pp. 32–38, 1957.

[115] F. Lin, S. E. Shelton, D. Espíndola, J. D. Rojas, G. Pinton, and P. A. Dayton, "3-D ultrasound localization microscopy for identifying microvascular morphology features of tumor angiogenesis at a resolution beyond the diffraction limit of conventional ultrasound," *Theranostics*, vol. 7, no. 1, pp. 196–204, 2017.

[116] V. Hingot, C. Errico, M. Tanter, and O. Couture, "Subwavelength motion-correction for ultrafast ultrasound localization microscopy," *Ultrasonics*, vol. 77, pp. 17–21, May 2017.

[117] J. Foiret, H. Zhang, T. Ilovitsh, L. Mahakian, S. Tam, and K. W. Ferrara, "Ultrasound localization microscopy to image and assess microvasculature in a rat kidney," *Sci. Rep.*, vol. 7, Oct. 2017, Art. no. 13662.

[118] K. Christensen-Jeffries, J. Brown, P. Aljabar, M. Tang, C. Dunsby, and R. J. Eckersley, "3-D *in vitro* acoustic super-resolution and super-resolved velocity mapping using microbubbles," *IEEE Trans. Ultrason., Ferroelectr., Freq. Control*, vol. 64, no. 10, pp. 1478–1486, Oct. 2017.
[119] S. Dencks, D. Ackermann, and G. Schmitz, "Evaluation of bubble tracking algorithms for super-resolution imaging of microvessels," in *Proc. IEEE Int. Ultrason. Symp. (IUS)*, Sep. 2016, pp. 1–4.
[120] A. Bar-Zion, C. Tremblay-Darveau, O. Solomon, D. Adam, and Y. C. Eldar. (2016). "Fast vascular ultrasound imaging with enhanced spatial resolution and background rejection." [Online]. Available: https://arxiv.org/abs/1601.05710
[121] C. Demené *et al.*, "4D microvascular imaging based on ultrafast Doppler tomography," *Neuroimage*, vol. 127, pp. 472–483, Feb. 2015.
[122] R. J. G. van Sloun, O. Solomon, Y. C. Eldar, H. Wijkstra, and M. Mischi, "Sparsity-driven super-localization in clinical contrast-enhanced ultrasound," in *Proc. IEEE Int. Ultrason. Symp. (IUS)*, Sep. 2017, p. 1.
[123] J. Zhan, X.-H. Diao, J.-M. Jin, L. Chen, and Y. Chen, "Superb microvascular imaging—A new vascular detecting ultrasonographic technique for avascular breast masses: A preliminary study," *Eur. J. Radiol.*, vol. 85, no. 5, pp. 915–921, 2016.
[124] K. Wei, A. R. Jayaweera, S. Firoozan, A. Linka, D. M. Skyba, and S. Kaul, "Quantification of myocardial blood flow with ultrasound-induced destruction of microbubbles administered as a constant venous infusion," *Circulation*, vol. 97, no. 5, pp. 473–483, 1998.
[125] D. Ghosh *et al.*, "Monitoring early tumor response to vascular targeted therapy using super-resolution ultrasound imaging," in *Proc. IEEE Int. Ultrason. Symp. (IUS)*, Sep. 2017, pp. 1–4.
[126] D. Ghosh *et al.*, "Super-resolution ultrasound imaging of the microvasculature in skeletal muscle: A new tool in diabetes research," in *Proc. IEEE Ultrason. Symp.*, Sep. 2017, pp. 1–4.
[127] G. P. Luke, A. S. Hannah, and S. Y. Emelianov, "Super-resolution ultrasound imaging *in vivo* with transient laser-activated nanodroplets," *Nano Lett.*, vol. 16, no. 4, pp. 2556–2559, 2016.
[128] P. S. Sheeran, S. Luois, P. A. Dayton, and T. O. Matsunaga, "Formulation and acoustic studies of a new phase-shift agent for diagnostic and therapeutic ultrasound," *Langmuir*, vol. 27, no. 17, pp. 10412–10420, 2011.
[129] V. Hingot *et al.*, "Subwavelength far-field ultrasound drug-delivery," *Appl. Phys. Lett.*, vol. 109, no. 19, p. 194102, 2016.
[130] N. de Jong, "Acoustic properties of ultrasound contrast agents," Ph.D. thesis, Erasmus Univ. Rotterdam, Rotterdam, The Netherlands, 1993.
[131] H. Koruk, A. El Ghamrawy, A. N. Pouliopoulos, and J. J. Choi, "Acoustic particle palpation for measuring tissue elasticity," *Appl. Phys. Lett.*, vol. 107, no. 22, p. 223701, 2016.
[132] R. W. Bourdeau *et al.*, "Acoustic reporter genes for noninvasive imaging of microorganisms in mammalian hosts," *Nature*, vol. 553, no. 7686, pp. 86–90, 2018.
[133] N. McDannold, N. Vykhodtseva, and K. Hynynen, "Blood-brain barrier disruption induced by focused ultrasound and circulating preformed microbubbles appears to be characterized by the mechanical index," *Ultrasound Med. Biol.*, vol. 34, no. 5, pp. 834–840, 2008.
[134] A. Bouakaz, A. Zeghimi, and A. A. Doinikov, "Sonoporation: Concept and mechanisms," in *Therapeutic Ultrasound* (Advances in Experimental Medicine and Biology), vol. 880, J. M. Escoffre and A. Bouakaz, Eds. Cham, Switzerland: Springer, 2016.

Olivier Couture was born in Quebec City, QC, Canada, 1978. He received the B.Sc. degree in physics from McGill University, Montreal, QC, Canada, in 2001, and the Ph.D. degree from the Department of Medical Biophysics, University of Toronto, Toronto, ON, Canada, in 2007.

After a Post-Doctoral Fellowship at ESPCI Paris, Paris, France, he was hired as a tenured Research Associate at CNRS, based within the Langevin Institute, Paris. His current research interests include ultrasound localization microscopy, ultrafast ultrasound imaging, drug delivery, velocipede oscillations, contrast agents, diabetes, and stroke.

Dr. Couture was awarded the "2017 IEEE Ultrasonics Early Career Investigation Award" for the development of ultrasound super-resolution and plane-wave contrast imaging and the Sylvia Sorkin Greenfield Award of the American Association of Physicists in Medicine for the Best Paper published in Medical Physics in 2011 and received the prestigious ERC Consolidator Grant for the application of ultrasound localization microscopy to medical diagnosis.

Vincent Hingot graduated from ESPCI Paris, Paris, France, in 2016, majoring in technologies for health, and started the Ph.D. degree with the Institute Langevin, Paris, with a focus on medical ultrasound with M. Tanter and O. Couture.

Following the work of C. Errico and M. Bézagu, he focused on exploiting different interactions between ultrasound and contrast agents for imaging and therapy, and ultrafast ultrasound localization microscopy and its application to the study of different vascular pathologies, together with the development of new techniques for ultrasound mediated drug delivery and its application to the delivery of anticancerous agents.

Baptiste Heiles was born in France in 1990. He received the M.Sc. degree in general and civil engineering from Ecole Normale Superieure Paris Saclay, Cachan, France, in 2013, the agrégation de Sciences Industrielles degree in 2014, and the Master of Research degree in fluid mechanics and heat transfers from Ecole Centrale de Paris, Châtenay-Malabry, France, in 2015.

Following the work of Y. Desailly and C. Errico, he focuses on exploiting contrast agents for imaging and implementing ultrasound localization microscopy (ULM) in volumetric imaging as well as improving ULM in conventional 2-D imaging.

Pauline Muleki-Seya received the M.S. degree in acoustics from the University of Le Mans, Le Mans, France, in 2011, and the Ph.D. degree in acoustics from the University of Lyon, Lyon, France, in 2014.

In 2015–2016 and 2016–2017, she was a Post-Doctoral Fellow at the Laboratory of Mechanics and Acoustics, Marseille, France, and at the Bioacoustics Research Laboratory, Department of Electrical and Computer Engineering, University of Illinois at Urbana–Champaign, respectively, conducting research on quantitative ultrasound techniques on soft tissues. Since 2017, she has been a Post-Doctoral Fellow at the Institut Langevin, Paris, France. Her current research interests include quantitative ultrasound techniques, ultrasound tissue, and microvasculature characterization and sonoporation.

Mickael Tanter received the Engineering degree from Supelec Gif-sur-Yvette, France, in 1994, and the Ph.D. degree in physics from the Paris 7 University, Paris, France, in 1999.

In 2006, he co-founded Supersonic Imagine, Aix-en-Provence, France, with M. Fink, J. Souquet, and C. Cohen-Bacrie. In 2014, he co-founded Cardiawave, Ile-de-France, France. In 2016, he co-founded Iconeus, Paris. He co-invented several major innovations in biomedical ultrasound, including transient elastography, ultrafast ultrasound, functional ultrasound imaging of brain activity, and ultrasound localization microscopy. Since 2016, he has been the Director of the first Technological Research Accelerator with the Institut National de la Santé Et de la Recherche Médicale (Inserm), Paris, dedicated to biomedical ultrasound, and created by Inserm to foster the translation of the laboratory's innovation into prototypes for biomedical research. He is currently a Research Professor with Inserm, and the Director of the Team Inserm U979 "Physics for Medicine" (Inserm/CNRS/ESPCI Paris). He has authored more than 220 peer-reviewed papers and book chapters, and holds 40 international patents.

Dr. Tanter is a member of the Technical Program Committee of the IEEE International Ultrasonics Symposium and the Administrative Committee of the IEEE UFFC Society. He received multiple international scientific distinctions, including the Grand Prize of the French Foundation for Medical Research in 2016, the Roberts Prize of Physics in Medicine and Biology for the best paper of the year 2015, and the Honored Lecture of the Radiology Society of North America in 2012. He was awarded with the prestigious European Research Council Advanced Grant in 2013 to develop functional ultrasound imaging and its applications. He is an Associate Editor of the IEEE TRANSACTIONS ON ULTRASONICS, FERROELECTRICS, AND FREQUENCY CONTROL.